Macromolecules
PERSPECTIVE

Macromolecules **2010**, *43*, 6515–6530 **6515**
DOI: 10.1021/ma100572e

Graphene/Polymer Nanocomposites

Hyunwoo Kim,[†] Ahmed A. Abdala,[‡] and Christopher W. Macosko*,[†]

[†]*Department of Chemical Engineering and Materials Science, University of Minnesota, Minneapolis, Minnesota 55455-0331, and* [‡]*Chemical Engineering Program, The Petroleum Institute, Abu Dhabi, United Arab Emirates*

Received March 15, 2010; Revised Manuscript Received June 14, 2010

ABSTRACT: Graphene has emerged as a subject of enormous scientific interest due to its exceptional electron transport, mechanical properties, and high surface area. When incorporated appropriately, these atomically thin carbon sheets can significantly improve physical properties of host polymers at extremely small loading. We first review production routes to exfoliated graphite with an emphasis on top-down strategies starting from graphite oxide, including advantages and disadvantages of each method. Then solvent- and melt-based strategies to disperse chemically or thermally reduced graphene oxide in polymers are discussed. Analytical techniques for characterizing particle dimensions, surface characteristics, and dispersion in matrix polymers are also introduced. We summarize electrical, thermal, mechanical, and gas barrier properties of the graphene/polymer nanocomposites. We conclude this review listing current challenges associated with processing and scalability of graphene composites and future perspectives for this new class of nanocomposites.

1. Introduction

Polymer nanocomposites based on carbon black, carbon nanotubes, and layered silicates have been used for improved mechanical, thermal, electrical, and gas barrier properties of polymers.[1−3] The discovery of graphene with its combination of extraordinary physical properties and ability to be dispersed in various polymer matrices has created a new class of polymer nanocomposites.

Graphene is an atomically thick, two-dimensional (2-D) sheet composed of sp^2 carbon atoms arranged in a honeycomb structure (Figure 1). It has been viewed as the building block of all other graphitic carbon allotropes of different dimensionality.[4] For example, graphite (3-D carbon allotrope) is made of graphene sheets stacked on top of each other and separated by 3.37 Å. The 0-D carbon allotrope, fullerenes (buckyballs), can be envisioned to be made by wrapping a section of graphene sheet. The 1-D carbon allotropes, carbon nanotubes (CNT) and nanoribbons, can be made by rolling and slicing graphene sheets, respectively. In reality, however, these carbon allotropes, with the exception of nanoribbons, are not synthesized from graphene. Graphite is a naturally occurring material with the first documented deposit[5] near Borrowdale, England, in 1555, but its first use may be dated back 4000 years.[6] Single-walled CNT (SWCNT) was first synthesized in 1991[7] following the discovery of fullerene in 1985.[8] Although the first reported method for production of graphene nanosheets can be traced back to 1970,[9] isolation of free-standing single-layer graphene was first achieved in 2004 when graphene was separated from graphite using micromechanical cleavage.[10]

With Young's modulus of 1 TPa and ultimate strength of 130 GPa, single-layer graphene is the strongest material ever measured.[11] It has a thermal conductivity of 5000 W/(m·K), which corresponds to the upper bound of the highest values reported for SWCNT bundles.[12] Moreover, single-layer graphene has very high electrical conductivity, up to 6000 S/cm,[13] and unlike CNT, chirality is not a factor in its electrical conductivity. These properties in addition to extremely high surface area (theoretical limit: 2630 m^2/g) and gas impermeability[14] indicate graphene's great potential for improving mechanical, electrical, thermal, and gas barrier properties of polymers.

Because of the great interest generated by the exceptional properties of graphene sheets and the discovery of methods for their production, researchers all over the world are studying graphene. This interest is clearly evident by the number of research publications. A simple search with *graphene* as a keyword using three of the most common databases—Institute for Scientific Information (ISI)-Web of Science, ScienceDirect, and SciFinder, as shown in Figure 2—indicates rapid growth of

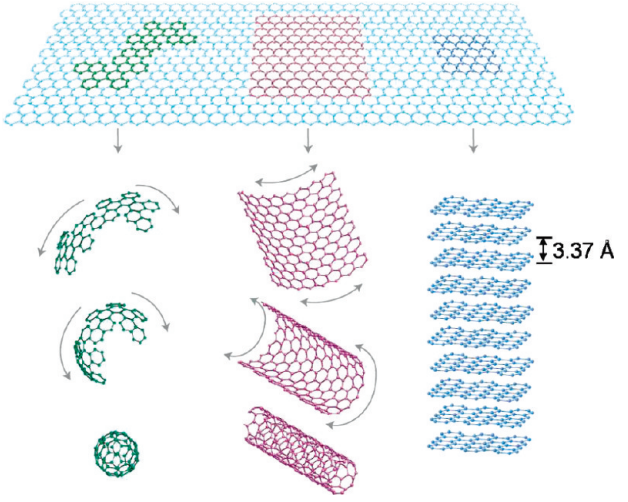

Figure 1. Graphene, the building block of all graphitic forms, can be wrapped to form the 0-D buckyballs, rolled to form the 1-D nanotubes, and stacked to form the 3-D graphite. Reproduced with permission from ref 4. Copyright 2007 Nature Publishing Group.

*Corresponding author: Tel +1 612-625-0092; Fax +1 612-626-1686; e-mail macosko@umn.edu.

Published on Web 07/23/2010

publications post 2005 with nearly 3000 publications in 2009. A similar trend in number of publications is also observed using *graphene composites* as a keyword.

In this paper, we review this literature with a focus on graphene/polymer composites. We first review the different methods for preparation of graphene sheets with an emphasis on methods suitable for polymer composite applications. Then methods to characterize graphene including number of layers, sheet size, and chemical modification are discussed. Dispersion routes for graphene into polymers and the resultant polymer/graphene composite properties are also reviewed. We conclude with challenges for future growth of this exciting new class of nanocomposites.

Hyunwoo Kim received his B.S. degree in chemical engineering from Seoul National University. After completing Ph.D. in chemical engineering with Professor Christopher W. Macosko at the University of Minnesota, he continued his research at Minnesota on processing, structure, and properties of graphene/polymer nanocomposites as a postdoctoral fellow. He will soon join the Dow Chemical Company as a Materials Processing Engineer.

Ahmed A. Abdala is assistant professor at the Chemical Engineering Department, The Petroleum Institute, Abu Dhabi, UAE. Dr. Abdala obtained his Ph.D. degree in Chemical Engineering and Fibers & Polymer Sciences from North Carolina State University in 2003. He also holds an M.S. in Chemical Engineering (North Carolina State University), M.S. in Petrochemicals, and B.S. in Petroleum Refining (Suez Canal University, Egypt). He is the inventor of the method for production of thermally reduced graphene (TRG). Along with his research interests on production, functionalization, and applications of graphene, Abdala's research focuses on rheology and applications of water-soluble polymers.

2. Bottom-Up Graphene

In bottom-up processes, graphene is synthesized by a variety of methods such as chemical vapor deposition (CVD),[15−21] arc discharge,[22,23] epitaxial growth on SiC,[24−30] chemical conversion,[31−33] reduction of CO,[34] unzipping carbon nanotubes,[35−37] and self-assembly of surfactants.[38] CVD and epitaxial growth often produce tiny amounts of large-size, defect-free graphene sheets. They may be more attractive than the mechanical cleavage method[10] for production of graphene sheets for fundamental studies and electronic applications but are not a suitable source for polymer nanocomposites that require a large amount of graphene sheets preferably with modified surface structure. The nature, average size, and thickness of the graphene sheets produced by different bottom-up methods as well as the advantages and disadvantages of each method are summarized in Table 1.

3. Top-Down Graphene

In top-down processes, graphene or modified graphene sheets are produced by separation/exfoliation of graphite or graphite derivatives (such as graphite oxide (GO) and graphite fluoride[39]). In general, these methods are suitable for large scale production required for polymer composite applications. Starting from graphite or its derivatives offers significant economic advantages over the bottom-up methods; graphite is a commodity material with current annual global production of over 1.1 million tons at $825/ton in 2008.[40] Therefore, the top-down approaches will be discussed in more detail. Figure 3 shows a block diagram which summarizes the different routes reported for production of graphene or modified graphene starting from graphite or GO.

Alkali metal[41]- or acid[42,43]-intercalated graphite can be expanded upon heat treatment to produce a thicker (∼100 nm) form of 2-D carbon known as expanded graphite (EG), which is commonly used as a filler for polymer composites. However, the

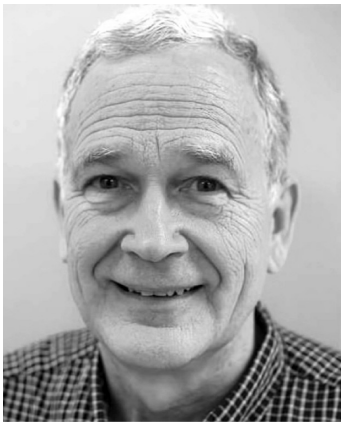

Chris Macosko is Director of the Industrial Partnership for Research in Interfacial and Materials Engineering and Professor of Chemical Engineering and Materials Science at the University of Minnesota and a member of the National Academy of Engineering. He received his B.S. from Carnegie Mellon, M.Sc. from Imperial College, London, and Ph.D. from Princeton. He has advised nearly 100 M.S. and Ph.D. students with whom he has published over 400 papers in rheology and polymer processing, particularly processing with reaction such as reaction injection molding, polyurethane foam, cross-linking, and reactive compatibilization of polymer blends.

layered structure of graphite is still maintained in EG.[44] Recently, a thinner form (~10 nm) of EG known as graphite nanoplatelets (GNP) was produced by either thermal expansion of fluorinated graphite intercalation compounds[45] or microwave radiation of acid-intercalated graphite followed by pulverization using ball milling or ultrasonication.[46,47] Because the large diameter and rigidity of graphite flakes are preserved in this process, even without complete exfoliation, GNP can improve electrical conductivity and mechanical properties of polymers at substantially smaller loadings than graphite or EG.[47,48] Properties of GNP reinforced polymers will be mentioned for comparison in section 6, but since the focus of this review is on single- or a few-layer graphene materials, GNP will not be discussed further.

3.1. Direct Exfoliation of Graphite. Micromechanical cleavage of graphite gave birth to the interest in graphene.[10] It can produce large-size, high-quality sheets but in very limited quantities, which makes it only suitable for fundamental studies or electronic applications.[10] However, recently graphite has also been directly exfoliated to single- and multiple-layer graphene via sonication in the presence of polyvinylpyrrolidone[49] or *N*-methylpyrrolidone,[50] electrochemical functionalization of graphite assisted with ionic liquids,[51] and through dissolution in superacids.[52] The direct sonication method has potential to be scaled up to produce large quantities of single- and multiple-layer graphene or functionalized graphene that can be used for composite applications. However, separation of the exfoliated graphene sheets from the bulk graphite could be a challenge. On the other hand, dissolution of graphite in chlorosulfonic acid[52] has potential for a large scale production, but the hazardous nature of the hydrosulfonic and the cost of its removal may limit this potential. Electrochemical exfoliation methods produce graphene sheets functionalized with imidazolium groups that assist dispersion in aprotic solvents.[51]

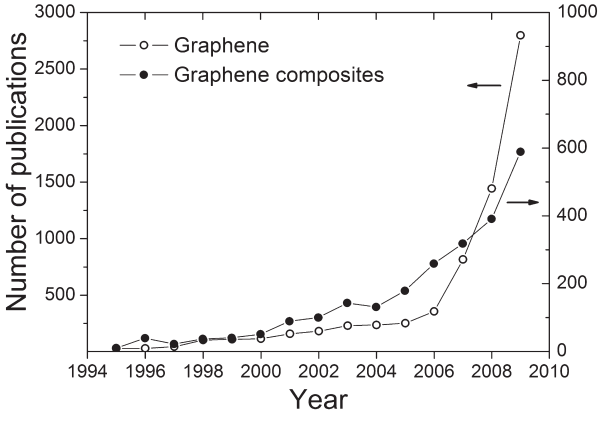

Figure 2. Number of publications returned using "graphene" and "graphene composites" as keywords in ISI-Web of Science, ScienceDirect, and SciFinder. Duplicates were removed.

3.2. Graphite Oxide (GO). Currently, the most promising methods for large scale production of graphene are based on the exfoliation and reduction of GO. GO was first prepared over 150 years ago by Brodie.[53] It is also produced using different variations of the Staudenmaier[54] or Hummers[55] methods in which graphite is oxidized using strong oxidants such as $KMnO_4$, $KClO_3$, and $NaNO_2$ in the presence of nitric acid or its mixture with sulfuric acid. Analogous to graphite, which is composed of stacks of graphene sheets, GO is composed of graphene oxide sheets stacked with an interlayer spacing between 6 and 10 Å depending on the water content.[56] The structure of graphene oxide has been the subject of theoretical[57−60] and experimental studies.[61−72] The Lerf−Klinowski model[66,67] is believed to be the most likely description of GO structure. The model describes GO as built of pristine aromatic "islands" separated from each other by aliphatic regions containing epoxide and hydroxyl groups and double bonds as shown in Figure 4a. Recently, Gao et al.[61] studied the structure of GO using ^{13}C NMR. They proposed that GO contains ketones, 6-membered lactol rings, and tertiary alcohol (Figure 4b) in addition to epoxide and hydroxyl groups. GO has an approximate C/O/H atomic ratio of 2/1/0.8.[53,73] During oxidation graphene oxide sheets undergo unzipping resulting in size reduction compared to the parent graphite flake size.[74] For more details about GO, we refer the reader to the extensive review of GO preparation, structure, and reactivity by Dreyer et al.[75]

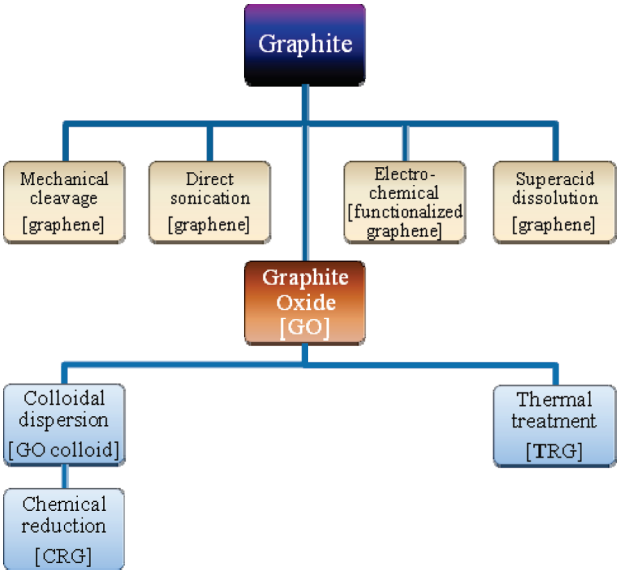

Figure 3. Top-down methods for production of graphene and modified graphene starting from graphite or via graphite oxide (GO).

Table 1. Bottom-Up Processes for Graphene Production

method	typical dimension: thickness	typical dimension: lateral	advantage	disadvantage	refs
confined self-assembly	single layer	100′s nm	thickness control	existence of defects	38
CVD	few layers	very large (cm)	large size; high quality	small production scale	15−21
arc discharge	single-, bi-, and few layers	few 100 nm to a few μm	can produce ~10 g/h of graphene	low yield of graphene; carbonaceous impurities	22, 23
epitaxial growth on SiC	few layers	up to cm size	very large area of pure graphene	very small scale	24−30
unzipping of carbon nanotubes	multiple layers	few μm long nanoribbons	size controlled by selection of the starting nanotubes	expensive starting material; oxidized graphene	35−37
reduction of CO	multiple layers	sub-μm	unoxidized sheets	contamination with α-Al_2O_3 and α-Al_2S	34

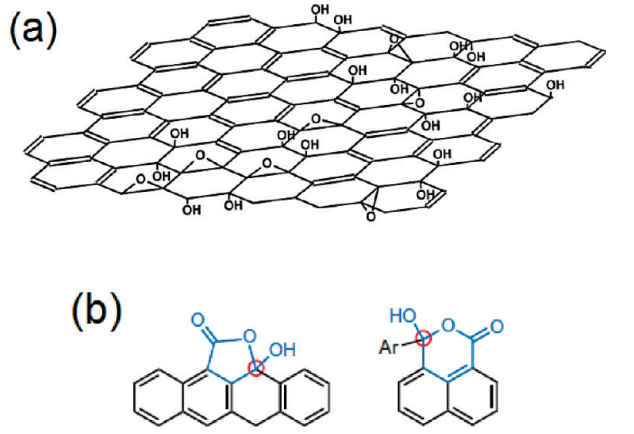

Figure 4. Structure of GO (a) consisting of aromatic islands separated by aliphatic regions containing oxygen bonded carbons as described by the Lerf−Klinowski model (image adopted and modified from ref 67) and (b) ketone groups in 6- and 5-membered ring as proposed in ref 61. The actual oxygen content of GO corresponds to C/O ratio of ~2, which is higher than what is shown in (a). This is due to the difficulty in representing bonds on the other side of the sheet and because a majority of C atoms on the edges (not shown) are O-substituted. Images were reproduced with permission.

Exfoliation of GO to produce chemically modified graphene sheets provides different routes for large scale production of functionalized graphene sheets. Although GO can be readily dispersed in water[76] and in organic solvents after chemical modification, graphene oxide is electrically insulating and thermally unstable. Therefore, at least partial reduction of graphene oxide is necessary to restore electrical conductivity. A number of different methods currently exist for the exfoliation and reduction of GO to produce chemically modified graphene. The term "chemically modified" is chosen because complete reduction of graphene oxide to graphene has not yet been observed. These methods are described in the following two sections. For more details about these routes, we refer the reader to Park and Ruoff's recent review.[56]

3.3. Chemical Reduction of GO. In these methods, a stable colloidal dispersion of GO is produced followed by chemical reduction of the exfoliated graphene oxide sheets. Stable colloids of graphene oxide can be obtained using solvents such as water, alcohol, and other protic solvents combined with either sonication or long stirring. Alternatively, GO can be exfoliated in polar aprotic solvents by reacting with organic compounds such as isocyanate[77] and octadecylamine[78] or treating with surfactants.[76,78,79] Although these suspensions can be used for production of GO/polymer composites, the low electrical conductivity and poor thermal stability of graphene oxide are significant drawbacks.

Colloidal graphene oxide or the organically treated version can be chemically reduced producing chemically reduced graphene (CRG) using hydrazine,[77,79,80] dimethylhydrazine,[81] sodium borohydride followed by hydrazine,[82] hydroquinone,[83] and UV-irradiated TiO_2.[84] Stankovich et al. proposed the following mechanism for reduction of graphene oxide using hydrazine:[77]

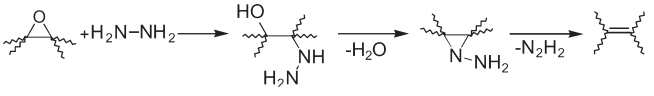

Reduction of graphene oxide restores electrical conductivity. However, significant oxygen content remains: C/O ~ 10/1.[76]

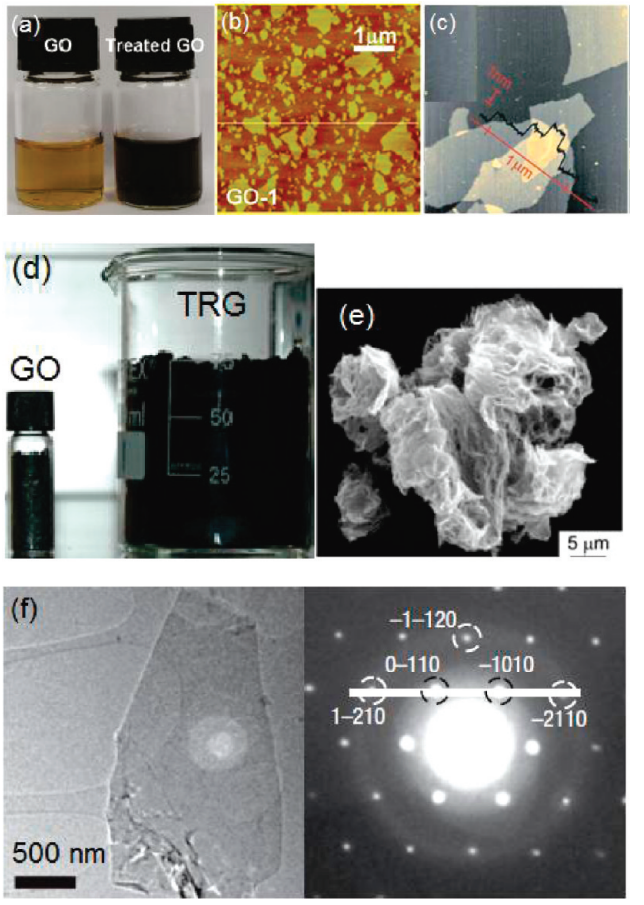

Figure 5. (a) GO suspension (0.5 mg/mL) before and after hydrothermal treatment at 180 °C;[85] (b, c) noncontact mode AFM images of GO on mica;[81,228] (d) 0.5 g of GO expands to 75 mL of TRG upon rapid heating to ~1000 °C; (e) SEM of TRG suggests a structure like crumpled sheets of paper,[90] and (f) TEM image of a single-layer graphene with an electron diffraction pattern with Miller−Bravais indices.[50] All images were reproduced with permission.

Although chemical reduction of graphene oxide provides an efficient route for production of CRG, the hazardous nature and cost of the chemicals used in reduction may limit its application. An alternative chemical reduction is dehydration of the hydroxyl groups on graphene oxide in water[85,86] at high pressure and temperature, 120−200 °C (Figure 5a). Aluminum powder appears to catalyze this process in an acidic condition.[87]

3.4. Thermal Exfoliation and Reduction. Thermally reduced graphene oxide (TRG) can be produced by rapid heating of dry GO under inert gas and high temperature.[88−91] Heating GO in an inert environment at 1000 °C for 30 s leads to reduction and exfoliation of GO, producing TRG sheets. Exfoliation takes place when the pressure generated by the gas (CO_2) evolved due to the decomposition of the epoxy and hydroxyl sites of GO exceeds van der Waals forces holding the graphene oxide sheets together. About 30% weight loss is associated with the decomposition of the oxygen groups and evaporation of water.[89] The exfoliation leads to volume expansion of 100−300 times producing very low-bulk-density TRG sheets (Figure 5d). Because of the structural defects caused by the loss of CO_2, these sheets are highly wrinkled as shown in Figure 5e.[89,90] 80% of the TRG sheets are single layers with an average size of about 500 nm independent of the starting GO size.[90] The advantage of the thermal reduction methods is the ability to produce chemically modified graphene sheets without the need for dispersion in a

Table 2. Top-Down Processes for Production of Graphene, Chemically Reduced (CRG), and Thermally Reduced Graphene Oxide (TRG)

method	typical dimension: thickness	typical dimension: lateral	advantage	disadvantage	ref
directly from graphite					
micromechanical exfoliation	few layers	μm to cm	large size and unmodified graphene sheets	very small scale production	10
direct sonication of graphite	single and multiple layers	μm or sub-μm	unmodified graphene; inexpensive	low yield; separation	49, 50
electrochemical exfoliation/ functionalization of graphite	single and few layers	500−700 nm	single step functionalization and exfoliation; high electrical conductivity of the functionalized graphene	cost of ionic liquids	51
superacid dissolution of graphite	mostly single layer	300−900 nm	unmodified graphene; scalable	use of hazardous chlorosulfonic acid; cost of acid removal	52
from graphite derivatives (graphite oxide (GO) or graphite fluoride)					
Li alkylation of graphite fluoride	single layer	μm	large size; functionalized sheets; no oxygen functionality	cost of the starting material; restacking after annealing	39
chemical reduction of colloidal GO in water	single and multiple layer CRG	μm or sub-μm size	large sheet size; some routes use only water	some of these methods use hazardous chemicals; only dispersed in hydrophilic polymers	77, 80, 82−87
chemical reduction of organically treated GO	mostly single layer CRG	few 100 nm to a μm	colloidal stability in organic solvents; better exfoliation	low thermal stability; in situ chemical reduction degrades some polymers	77−79
thermal exfoliation/reduction of GO	single and few layer TRG	~500 nm	1-step exfoliation/reduction; short heating time; dry basis	high heating temperature; smaller sheet size compared to chemically reduced sheets	89, 90

solvent. TRG has C/O ratio of about 10/1 compared to 2/1 for GO.[90] This ratio has been increased up to 660/1 through heat treatment at higher temperature (1500 °C) or for longer time.[92] TRG sheets have high surface area, 1700 m^2/g, as measured in methylene blue and can be well dispersed in organic solvents such as *N,N*-dimethylformamide (DMF) and tetrahydrofuran. The thermal reduction also leads to restoration of the electrical conductivity with reported electrical conductivity of a compacted film with density 0.3 g/cm^3 ranging between 10 and 20 S/cm,[89] compared to 6000 S/cm for defect-free single graphene sheets.[13]

The nature, average size, and thickness of the graphene sheets produced by different top-down methods as well as the advantages and disadvantages of each method are summarized in Table 2. As indicated in the discussion above and in the table, the most promising routes to preparation of graphene for polymer nanocomposites start from GO. Thus, in the rest of this Perspective we will concentrate on these routes.

4. Characterization of Graphene

It is important to verify that the synthesis methods described above do in fact produce graphene single sheets. Moreover, the size of these sheets and attached functional groups are important for dispersion in polymers. In this section we review briefly the techniques best suited for characterization of graphene sheets.

4.1. Layer Number and Size. X-ray diffraction is used to demonstrate that graphite has been intercalated. For example, the sharp reflection at $2\theta = 26.3°$ (Cu Kα radiation, X-ray wavelength = 0.154 nm) in graphite shifts to 14.1°−14.9° in graphite oxide.[64] However, X-ray diffraction disappears as the sheets of GO exfoliate into single sheets.[89,90]

Although indirect, surface area has been used as an indicator of exfoliation. Since theoretically the specific surface area is inversely proportional to thickness of disk-like particles, (~2/density/thickness), well-exfoliated sheets will have higher surface area. Surface area can be determined by N_2 or methylene blue adsorption.[89,90] However, Schniepp et al.[89] noted that N_2 adsorption measurements were highly dependent on the compressibility of TRG. Although methylene blue adsorption is done on exfoliated sheets in solution and thus avoids compressibility issues, surface topology and chemistry may influence the area occupied by each methylene blue molecule.

Atomic force microscopy (AFM) imaging provides more reliable measures of sheet dimensions. Contact or tapping mode AFM can be used to probe surface topology, defects, and bending properties.[89,93] Lateral size and layer thickness of particles lying on substrates can be determined from the steps in height scans as illustrated in Figure 5b,c. Folded[93] or wrinkled sheets[72,89] as well as adsorbed solvents or moisture[77,94] can complicate measurements. Scanning electron microscopy (SEM) can give qualitative insight into the three-dimensional structure of graphene sheets as illustrated in Figure 5e.[90]

Figure 5f shows a transmission electron microscopy (TEM) image of a single graphene sheet on a holey carbon-covered copper grid.[50] In addition to size determination by TEM imaging, electron diffraction patterns can clearly differentiate single from bilayer sheets.[95] High-resolution TEM (HR-TEM) can identify atomic bonds on functionalized sheets (C−OH vs C−O−C) and atomistic defects.[72] HR-TEM has also confirmed the existence of aliphatic islands containing oxygen bonded carbons as proposed in Figure 4a.

Size and morphology of platelets can be estimated indirectly in dilute solution. Viscosity measurements of suspensions in the dilute limit do not have orientation problems and can give particle aspect ratio. Pasquali and co-workers[96] have used intrinsic viscosity measurements to evaluate average length of surfactant stabilized SWCNT in water assuming rigid rods, but as yet, intrinsic viscosity has not been applied to characterize graphene. Static light scattering from

Table 3. Electrically Conductive Graphene/Polymer Nanocomposites

polymer[a]	graphene type	processing	electrical percolation threshold (vol %)	ref
		chemically modified		
PS	iGO[b]	solvent blending + hydrazine	0.1	81
vinyl chloride/vinyl acetate copolymer	GO	solvent blending + hydrazine	0.15	142
PS	electrochemically exfoliated graphite	solvent blending + ionic liquid	0.13−0.37	51
epoxy	partially reduced GO	in situ polymerization at 250 °C	0.52	147
PMMA	GO (17 mol % O)	in situ polymerization	(1.3)[c]	116
PMMA	GO (12 mol % O)	in situ polymerization	(1.6)	144
		thermally exfoliated		
TPU	TRG, ~800 m^2/g, 4 mol % oxygen	solvent blending	0.3	112
		in situ polymerization	0.4	
		melt compounding	0.8	
PEN		melt compounding	0.5	125
PC		melt compounding	0.6	124
natural rubber	> 600 m^2/g, 5 mol % oxygen	melt or solvent blending + vulcanization	(0.8, solvent blend), (> 2.0, melt blend)	123
PS−PI−PS		melt or solvent blending	(0.6)	
PDMS		oligomer blending + polymerization	(0.6)	
TPU	apparent specific volume: 410 cm^3/g, 5 mol % oxygen	solvent blending	(1.0)	145
TPU		solvent blending	(1.0)	146
TPU		in situ polymerization	(1.6)	120
PVDF	−	solvent blending	(1.6)	143
SAN	600−950 m^2/g, up to 14 mol % oxygen	preblending using solvents, followed by melt compounding	(1.9)	91
PC			(1.3)	
PP			(2.0)	
PA6			(3.8)	

[a] PS: polystyrene; PMMA: poly(methyl methacrylate); TPU: thermoplastic polyurethane; PEN: poly(ethylene-2,6-naphthalate); PC: polycarbonate; PS−PI−PS: poly(styrene-*co*-isoprene-*co*-styrene) triblock copolymer; PDMS: polydimethylsiloxane; PVDF: poly(vinylidene fluoride); SAN: poly(styrene-*ran*-acrylonitrile); PP: polypropylene; PA6: polyamide 6. [b] Isocyanate-treated graphite oxide. [c] Values in parentheses are percolation volume fraction converted from the weight fraction reported using density of the polymer and graphite (2.28 g/cm^3).

dilute GO in water can give fractal dimensions d_f of GO. One study showed nearly flat sheets ($d_f = 2.15$)[97] while another reported GO as crumpled membranes (2.54).[98] However, the results were sensitive to solvent polarity: GO collapsed to a compact structure upon addition of acetone leading to higher fractal dimension.[97,98]

4.2. Identifying Chemical Modification. As indicated in Table 2, the routes most suitable for producing graphene sheets in large quantities start from GO, and thus all have some remaining oxygen. The overall degree of oxidation can be quantified by standard elemental analysis. X-ray photoelectron spectroscopy (XPS) can quantify the amount of oxygen on the surface and also indentify the types of carbon oxygen bonds. Chemical shifts in XPS C_{1s} spectra can be evidence for existence of C−O, C═O, or O−C═O on GO and its derivatives[76,77,99] but are limited in quantifying their relative amounts. Infrared absorption[100−102] has similar limitations. ^{13}C NMR may be the most direct method to distinguish oxygen functional groups.[61,64,66] However, since the NMR-active ^{13}C allotrope occurs naturally at only ~1%, signal-to-noise ratio is low. By CVD of ^{13}C-labeled graphene on nickel substrates and subsequent oxidation, Ruoff and co-workers[63] enhanced the signal and identified chemical groups and their connectivity.

Raman spectroscopy can quantify the transformation of sp^3-hybridized carbons back to sp^2 on reduction of GO[77,103] and the presence of disordered stacking in graphite samples.[104] The transformation of sp^3 to sp^2 restores electrical conductivity; thus, conductivity is also a valuable qualitative measure of the conversion of graphene oxide to graphene.[77,99,105,106]

5. Dispersion of Graphene into Polymers

The properties of polymer nanocomposites depend strongly on how well they are dispersed. Much of nanocomposite research with carbon nanotubes (CNT) has focused on finding better methods for dispersing nanotubes into polymers.[2] Surface functionalization via fluorination,[107] acid modification,[108] and radical addition[109] improves solubility of CNT in solvents and polymers. However, disentangling the bundles during dispersion into polymers cannot be done easily, and sonication often shortens the tubes. The synthesis of graphene from graphene oxide leaves some epoxide and hydroxyl groups; these greatly facilitate functionalization.[73,78,79,81] Since graphene oxide and CRG are flat sheets, entangled bundles are not an issue. However, restacking of the flat sheets, especially after chemical reduction, can significantly reduce their effectiveness. Restacking can be prevented by either use of surfactants that can stabilize the reduced particle suspensions[76] or blending with polymers prior to the chemical reduction.[81]

GO readily exfoliates in water or other protic solvents via hydrogen-bonding interaction.[97,98] Nanocomposites have been created with GO and water-soluble polymers such as poly(ethylene oxide) (PEO)[110] or poly(vinyl alcohol) (PVA).[111] Using GO after chemical modification with isocyanate or amine, composites have also been produced in aprotic solvents with hydrophobic polymers such as polystyrene (PS),[81] polyurethane (PU),[112,113] or poly(methyl methacrylate) (PMMA).[114] As discussed in section 3.3, electrical conductivity can be restored via chemical reduction of the graphene oxide. This can also be done in situ in the presence of a polymer. For example,

Table 4. Mechanical Properties of Graphene/Polymer Nanocomposites

polymer[a]	reinforcements	processing	E_{matrix} (MPa)	graphene concentration (vol %)	modulus increase (%)	tensile strength increase (%)	ultimate strain increase (%)	ref
PVA	GO	solvent	2100	2.5	128	70	32	183
PVA	GO	solvent	2130	(0.49)[b]	62	76	−70	224
PMMA	GO	in situ polymerization	520[c]	(1.7)	54[c]	N/A	N/A	116
PCL	GO	solvent	340	(2.4)	108	36	−90	176
PCL	GO	solvent	260	(0.46)	50	N/A	N/A	177
epoxy	TRG	in situ polymerization	2850	(0.05)	31	40	N/A	172
PEN	TRG	melt	2350	2.4	57	N/A	N/A	125
PC	TRG	melt	2080	1.3	25	N/A	N/A	124
PMMA	TRG	solvent	2100	(0.005, 0.5)	33, 80	N/A	N/A	173
PVDF	TRG	solvent	1280	(3.1)	92	N/A	N/A	143
SAN	TRG	solvent + melt	2350	(2.3)	34	N/A	−58	91
PC			1480	(2.5)	52	N/A	−98	
PP			980	(1.9)	43	N/A	−99	
PA6			1650	(2.4)	32	N/A	−94	
natural rubber	TRG	solvent/melt	1.3	(1.2)	750	N/A	N/A	123
PDMS		in situ polymerization	0.6	(2.2)	1100	N/A	N/A	
styrene−butadiene rubber		−	10	(0.8)	390	N/A	N/A	
TPU	TRG	solvent	458	(1.5)	43	−23	−15	146
silicone foam	TRG	in situ polymerization	250[d]	(0.12)	200[d]	N/A	N/A	119
PVA	acid functionalized TRG	solvent	660	(0.4)	35	N/A	N/A	114
PMMA	amine treated, acid functionalized TRG		2120	(0.3)	70	N/A	N/A	
TPU	TRG	melt	6.1−7.1	1.6	250	N/A	N/A	112
		solvent		1.6	680	N/A	N/A	
		in situ polymerization		1.5	210	N/A	N/A	
	iGO	solvent		1.6	490−900	N/A	N/A	
PS	PS-functionalized, chemically reduced GO	solvent	1450	(0.4)	57	N/A	N/A	225
TPU	chemically reduced sulfonated-graphene	solvent	9.8	(0.5)	120	75	N/A	113
TPU	GO	solvent	6	(2.4)	900	−19	−60	226
PAN	exfoliation of alkali intercalated graphite	electrospinning, solvent	2450	(2.1)	100	N/A	N/A	227

[a] PVA: poly(vinyl alcohol); PCL: polycaprolactone. [b] Values in parentheses are percolation volume fraction estimated from the weight fraction reported using density of the polymer and graphite (2.28 g/cm^3). [c] Measured at 60 °C. [d] Compressive modulus, normalized by relative polymer density.

Stankovich et al. added sulfonated polystyrene and then reduced graphene oxide with hydrazine hydrate.[76] Without the sulfonated polystyrene, the reduced sheets rapidly aggregated. However, depending on polymer type and the reducing agent, this in situ reduction technique may result in polymer degradation.

Composites of CRG and TRG have been made with a number of polymers via blending with organic solvents followed by solvent removal. Unlike chemically modified GO that retains some layered structure from GO, thermal expansion of GO (TRG) leads to nearly complete exfoliation.[89,90] Therefore, dispersion of TRG can be easier while stacked layers of CRG have to be exfoliated by applying mechanical stress and via intergallery polymer diffusion in solvents.[112] Because of its wrinkled structure, TRG may experience less restacking after solvent removal than the flatter CRG sheets.

Graphene composites can be produced via in situ intercalative polymerization of monomers. Successful polymerizations of PVA,[115] PMMA,[116] epoxy,[117] and poly(arylene disulfide)[118] with graphene oxide or silicone foams[119] and PU[112,120] with TRG have been reported. Especially for poly(arylene disulfide), graphene oxide was used as an oxidation agent which converts thiol salts to disulfide. However, so far monomers have only been polymerized in solvents. The high viscosity of even dilute dispersion of graphene makes bulk-phase polymerization difficult. If functional groups on the chemically modified graphene are reactive with the monomer, grafting of polymer chains onto graphene surfaces can occur. Chain grafting has been demonstrated with the polymerization of poly(2-(dimethylamino)ethyl methacrylate)[121] and PVA[122] and with PU formation.[112]

The most economically attractive and scalable method for dispersing nanoparticles into polymers is melt blending. However, because of thermal instability of most chemically modified graphene, use of melt blending for graphene has so far been limited to a few studies with the thermally stable TRG. Successful melt compounding of TRG into elastomers[112,123] and glassy polymers[124,125] has been reported. In the few direct comparisons between solvent and melt blending,[112] solvent blending produces better dispersion (Tables 3, 4, and 5). Another challenge for melt compounding is the low bulk density of graphene like TRG, which makes feeding into melt mixers difficult. Torkelson and coworkers[126] have attempted to bypass all graphene synthesis steps by exfoliating graphite directly into polypropylene using the very high stresses generated in the solid-state shear pulverization process. Their X-ray diffraction and TEM data indicate, however, that the resulting composite is primarily small stacks of graphite.

Table 5. Gas Permeability of Graphene/Polymer Nanocomposites

polymer	filler	processing	permeant	relative reduction (%)	graphene loading (vol %)	ref
PEN	TRG	melt	hydrogen	44	1.8	125
PC	TRG	melt	helium	32	1.6	124
			nitrogen	39	1.6	
TPU	TRG	melt	nitrogen	52	1.6	112
		solvent	nitrogen	81	1.6	
		in situ polymerization	nitrogen	71	1.5	
	iGO	solvent	nitrogen	94−99	1.6	
	GO	in situ polymerization	nitrogen	62	1.5	
natural rubber	TRG	melt/solvent/oligomer polymerization	air	60	1.7	123
PS−PI−PS				∼80	2.2	
PDMS				∼80	2.2	

5.1. Quantifying Dispersion. Most studies have relied on improved physical properties to demonstrate that their graphene is well dispersed in the polymer matrix. These indirect methods will be reviewed in the next section. However, TEM can give direct images of dispersion and has been widely used to visualize layered silicates in polymers.[127,128] Graphite can be imaged in TEM without staining[91,112,125] although it has a lower atomic number contrast with polymers than layered silicates. The smaller thickness of isolated graphene sheets (∼0.34 nm) makes them more difficult to be resolved in TEM micrographs. Moreover, functionalization and defects formed during thermal exfoliation distort flat graphene into highly wrinkled sheets. In an extensive study of TEM images of layered silicates/polymer nanocomposites, Fornes and Paul[128] discuss other difficulties in using TEM to quantify the dispersion of thin platelike fillers.

Despite these difficulties, there has been at least one attempt to quantify graphene dispersion embedded in polymers directly with TEM. Figure 6 highlights the difference between graphite and TRG dispersed in poly(ethylene naphthalate) (PEN).[125] The wrinkled nature of TRG can be seen in some of the sheets in Figure 6b. A measure of dispersion is the aspect ratio of the particles, A_f = (sheet length)/thickness. Using similar micrographs, sheet lengths were evaluated by drawing straight contour lines as shown in Figure 6b. Thickness was determined from full width at half-maximum of a linear intensity profile crossing each particle. Values for ∼100 sheets are plotted in Figure 6c. Despite the possibility of missing thinner layers, the distribution of these aspect ratios is a useful measure of TRG dispersion.

5.2. Rheology. Rheology can be an effective tool for quantifying nanocomposite dispersion.[129] It averages over many particles and is also useful in its own right for predicting processability. An experiment that can yield A_f is the onset of network formation. Figure 7 shows the shear storage modulus, G', from small strain oscillatory shear versus frequency for a series of concentrations of graphite and TRG dispersed in PEN at 290 °C.[125] At about 5 wt % graphite and 1 wt % TRG, G' becomes independent of frequency at low frequency, a signature of solidlike network formation. In this rigidity percolation regime, the concentration ϕ dependence of the elasticity of particle suspensions can be described by power law scaling[129,130]

$$G' \propto (\phi - \phi_{perc})^{\nu} \quad (1)$$

where ϕ_{perc} is the percolation threshold and ν is a power-law exponent. ϕ_{perc} of graphene can be determined experimentally from a plot of low-frequency G' versus $\phi - \phi_{perc}$. Compared with spheres, particles with shape anisotropy (disks and rods) percolate at smaller volume fraction.[131,132] In extreme oblate/prolate limits, the percolation threshold is inversely proportional to the particle aspect ratio. With a few simplifying assumptions (randomly oriented, monodispersed, and disk-shaped particles), Ren et al.[133] identified a proportionality between A_f and ϕ_{perc}

$$A_f = \frac{3\phi_{sphere}}{2\phi_{perc}} \quad (2)$$

where $\phi_{sphere} = 0.29$, the onset of percolation of interpenetrating, randomly packed spheres.[134] Using the data of Figure 7 to determine ϕ_{perc}, eq 2 gives $A_f = 18$ for graphite, in good agreement with the TEM results in Figure 6c. For TRG, $A_f = 160$, considerably higher than the value determined from the electron micrographs. At least part of this difference may be due to TEM missing the thinnest sheets as discussed above. The percolation threshold for electrical conductivity (see Table 3) can also be used to quantify dispersion through A_f. From the electrical percolation values, $A_f \sim 13$ for graphite in PEN and ∼100 for TRG. The higher values of A_f (160) calculated using G' data may indicate that polymer chains can bridge between particles

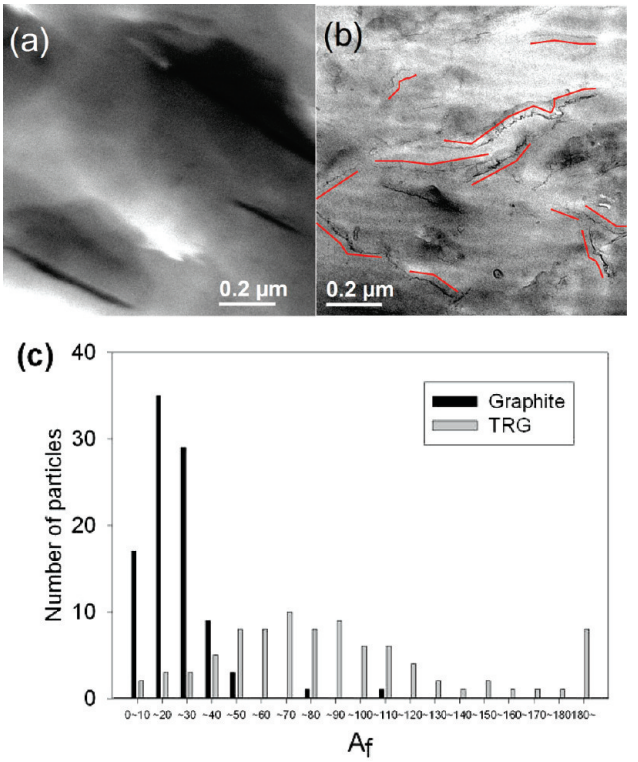

Figure 6. Comparison of the dispersion of graphite and TRG at 3 wt % in PEN by TEM: (a) graphite and (b) TRG. Solid lines indicate lengths used to evaluate aspect ratio, A_f. (c) Aspect ratio distribution from measurements on several micrographs. Average A_f = 21 (graphite) and 88 (TRG).[125] Images were reproduced with permission.

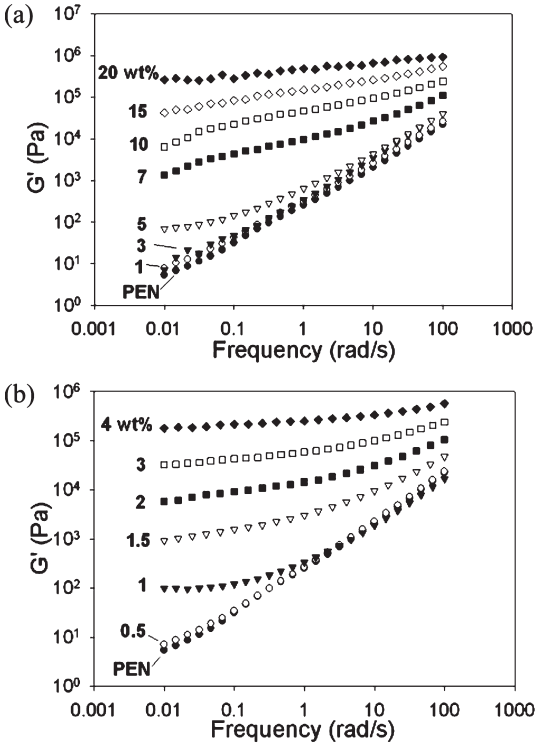

Figure 7. Dynamic frequency sweeps of PEN containing (a) graphite and (b) TRG at 290 °C. Adopted from ref 125.

causing network percolation at a lower concentration than conductivity percolation.[135]

However, there are several limitations in using rheological measurements to quantify graphene dispersion. Rheological responses are sensitive to the orientation of anisotropic particles.[135,136] Typical analyses assume random particle orientation which can be far from the fact since processing and even loading into a rheometer induce particle alignment, especially for high aspect ratio particles concentrated in viscous polymer matrices. For example, 1 wt % TRG was dispersed in a polycarbonate (PC) melt matrix of viscosity 4000 Pa·s.[124] Its elastic shear modulus showed no sign of reaching equilibrium even 10 h after loading the sample into the rheometer at 230 °C. Brownian randomization was extremely slow under typical experimental conditions.[137] Similar temporal changes in melt viscoelasticity and also electrical conductivity through annealing were reported from layered silicates,[137] CNT,[138] and carbon nanofiber (CNF)[139] composites. Although meaningful results can be obtained if time after loading is held constant, sufficient thermal stability of the matrix is required for prolonged rheological tests.

6. Properties of Graphene/Polymer Nanocomposites

As reviewed in the previous sections, exfoliated carbon sheets obtained from graphene oxide (GO) via either chemical reduction or rapid pyrolysis can be dispersed in polymers to modify their physical properties. In this section, we present electrical, thermal, mechanical, and gas barrier properties of graphene/polymer nanocomposites.

6.1. Electrical Conductivity. Graphene sheets can provide percolated pathways for electron transfer, making the composites electrically conductive. Similar benefits can be achieved with other conductive carbon fillers such as carbon black (CB), carbon nanofibers (CNF), and expanded graphite. However, graphene enables the insulator to conductor

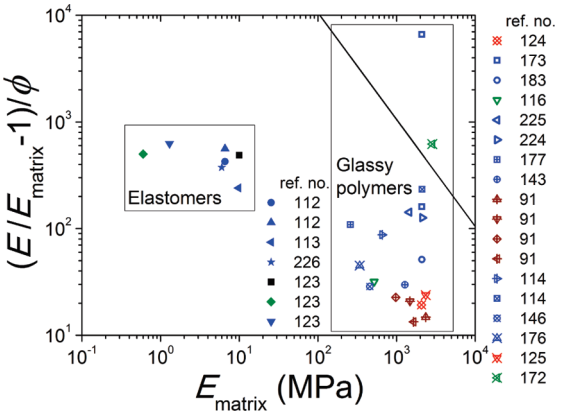

Figure 8. Relative modulus increase for polymer/graphene nanocomposites normalized by volume fraction of graphene as a function of matrix stiffness. Solvent blended, melt blended, and in situ polymerized composites are represented by blue, red, and green symbols, respectively. Brown symbols represent composites produced via preblend formation in solvent, followed by melt blending.[91] The diagonal solid line represents the Voigt limit, infinitely long sheets all aligned in the tensile direction.

transition at significantly lower loading,[91] comparable to electrical percolation thresholds for carbon nanotubes (CNT). When particles possess the same aspect ratio, theory[131] predicts that prolates (rod-like) percolate at one-half the volume fraction of oblates (disk-like). However, since real composite morphology is rather complex (particle interaction, flexibility, and entanglement), this does not apply in reality: rod-like CNT may not necessarily percolate at lower concentration than disk-like graphene. Particle orientation also plays an important role: the percolation threshold becomes greater as particles are aligned parallel.[140,141]

Production of electrically conductive polyolefin,[91] vinyl[51,81,91,115,142,143] and acrylic[116,144] polymers, polyester,[91,124,125] polyamide,[91] polyurethane,[112,145,146] epoxy,[147] natural and synthetic rubbers[123] with graphene has been reported. These materials can be used, for example, for electromagnetic shielding,[147,148] antistatic coating, and conductive paints.[149] Table 3 shows the wide range of electrically conductive polymer/graphene composites, their production methods, and minimum filler volume fraction for electrical conduction. When electrical percolation thresholds were provided only in weight fraction, they were converted to the volume fraction (values in parentheses in Tables 3, 4, and 5) using density of the polymer[150] and graphite, 2.28 g/cm^3.[125]

The lowest electrical percolation threshold was 0.1 vol % reported by Stankovich et al.[81] for PS solvent blended with isocyanate-treated GO (iGO)[94] followed by solution-phase reduction with dimethylhydrazine. This onset of percolation is comparable with those of SWCNT or multiwalled carbon nanotubes (MWCNT).[2] Also, electrochemical exfoliation of graphite in ionic liquids is reported to produce graphitic layers that can percolate at 0.13−0.37 vol % in PS.[51]

As mentioned in sections 3 and 5, thermally reduced graphene (TRG)[89] retains high conductivity without additional reduction steps and can be melt processed due to its thermal stability. However, for thermoplastic polyurethane (TPU),[112] films cast from a DMF solution still showed better dispersion of these carbon sheets and required lower loading for electrical conduction (0.3 vol %) than films compression-molded after melt compounding (0.8 vol %). The dispersion state of TRG and electrical conductivity of the composites may also vary depending on thermal exfoliation conditions and compatibility with the polymer matrix. Steurer et al.[91]

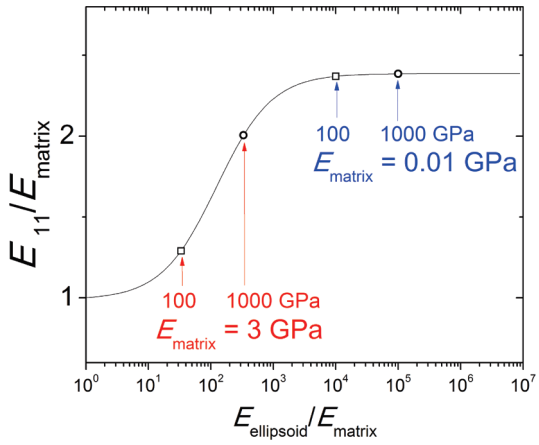

Figure 9. Relative increase in tensile modulus predicted by the theory of Mori and Tanaka[174,175] of elastomeric (E_{matrix} = 0.01 GPa) and glassy (3 GPa) polymer composites reinforced with ellipsoids (graphene), 1 vol % A_f = 200. Reducing ellipsoid stiffness $E_{ellipsoid}$ from 1000 (circles) to 100 GPa (squares) barely affects modulus enhancement for elastomers but almost eliminates it for glassy polymers.

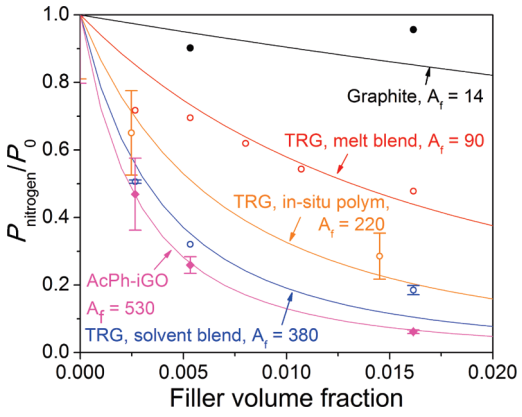

Figure 10. N_2 permeability of TPU composites normalized by permeability P_0 of neat TPU reproduced from ref 112. Gas permeation of TRG/TPU composites produced via melt, solvent mixing, and in situ polymerization are compared. AcPh-iGO represents acetylphenyl isocyanate-treated GO. Solid curves are predictions based on Lape et al.[182]

found percolation thresholds of TRG ranged from 1.3 to 3.8 vol % for different polymers even though processed using similar procedures (also see Table 3). Kim and Macosko[124] reported electrical percolation of TRG takes place in PC at ~0.6 vol %, notably lower than Steurer. This difference may be due to the fact that Steurer et al. used relatively milder conditions (~600 °C) for the rapid pyrolysis of GO. Orientation of anisotropic graphitic disks[124] also plays an important role, which can be induced by flow during processing: compression-molded TRG/PC composites are less conductive than samples annealed for long time.

It should be noted that Drzal and co-workers report that electrical percolation of polypropylene (PP) can be achieved at as low as 0.1−0.3 vol % with GNP derived from thermal expansion of acid-intercalated graphite.[47,48] GNP is not graphene; it still maintains the multilayer structure of graphite and relatively low specific surface area (~100 m^2/g).[151] However, its large particle aspect ratio (100−1500) and high rigidity of stacked sheets prevent particle buckling which might reduce the amount of particles necessary for electrical percolation. Surprisingly, for GNP in linear low-density polyethylene (PE), a polymer with very similar polarity to PP, electrical percolation was reported to be significantly higher, 12−15 wt %.[152] In the PP study, polymer pellets were coated with GNP from solvents prior to blending.[47] This strategy may break particle aggregates and improve the dispersion quality.

6.2. Thermal Conductivity. Superior thermal transport properties of graphene dispersion have potential for thermal management in miniaturized electronic devices,[117,153,154] for thermal pastes,[155] and for heat-actuated, shape-memory polymers.[113] It has been reported that 2-D, platelet-like GNP can improve thermal conductivity more effectively than 1-D, rod-like CNT or CNF.[156−159] However, unlike the exponential increase in electrical conductivity, thermal conductivity enhancement by the carbon nanofillers is not as dramatic,[158] even lower than expected from effective medium theory.[160] This is partly due to smaller contrast in thermal conductivity between polymers (0.1−1 W/(m·K)) and graphitic carbons (MWCNT[161] 3000 and graphene[12] 5000 W/(m·K)) compared to the contrast in electrical conductivity (graphene[13] 6000 and nonconducting polymers 10^{-18}−10^{-13} S/cm). Moreover, since thermal energy is transferred mainly in the form of lattice vibration (phonons), poor coupling in vibration modes at the filler−polymer and filler−filler[162] interfaces will impart significant thermal resistance (Kapitza resistance).[163] Huxtable et al. estimated thermal resistance at the CNT/polymer interface is equivalent to that of 20 nm thick polymer layers.[160] Matching surface chemistries[164] or covalent interface coupling[165] can be pursued to minimize the interfacial phonon scattering. However, excessive functionalization also tends to reduce the intrinsic thermal conductivity of carbon materials.[166]

Improving thermal conductivity using GNP was demonstrated for epoxy,[159,167,168] PP,[151] PE,[169] polyamide (PA),[169] and paraffin wax.[170] For epoxy, up to 30-fold increase in thermal conductivity was attained by incorporating 33 vol %[167] or 25 vol %[159] of few nanometer thick graphite platelets via solution polymerization. However, thermal conductivity increase for PP, PE, and PA composites via melt compounding with similar amount of GNP was less significant (less than 15-fold increase).[151,169] Degree of exfoliation, orientation, and interfacial interaction have an influence on the thermal transport in composites. Haddon and co-workers controlled A_f of GNP through choosing different thermal expansion temperatures and reported higher thermal conductivity increase for higher A_f of reinforcing platelets.[159] When the platelets are oriented by extrusion or solvent casting, conductivity was higher in the direction of graphite alignment than perpendicular implying macroscopic anisotropy.[157,167] Silane modification of EG[168] was used to enhance the conductivity gain for an epoxy; covalent bonding between graphite surface and polymer matrix may reduce the acoustic phonon scattering at the interface. For graphene oxide, strong interaction of surface −OH and −O− groups with epoxy resins enabled 4-fold increase in thermal conductivity at 5 wt %,[117] which can be compared with the performance of SWCNT. Also, TRG increased thermal conductivity of silicone foams[119] by 6% at 0.25 wt % although part of the conductivity increase may be attributed to the foam density increase (higher solid content) by graphene addition.

6.3. Mechanical Properties. Defect-free graphene is the stiffest material ($E \sim 1$ TPa) ever reported in nature and also has superior intrinsic strength, ~130 GPa.[11] Despite some structural distortion, the measured elastic modulus of CRG sheets is still as high as 0.25 TPa.[171] Advantages of graphene in mechanical reinforcement over existing carbon fillers such as CB, EG, and SWCNT have also been discussed.[91,123,172,173]

Table 4 is a summary of mechanical properties of graphene reinforced polymer nanocomposites. While modulus increase

with graphene dispersion is evident for all polymers, it is more pronounced for elastomeric matrices. This is due to greater stiffness contrast between reinforcement and matrix. This difference is more clearly illustrated in Figure 8, where we have plotted relative modulus E gains normalized by filler volume fraction, $(E/E_{matrix} - 1)/\phi$ versus neat matrix modulus, E_{matrix}. For glassy polymers, the most surprising results were found from PMMA (33% improvement at only 0.01 wt %)[173] and epoxy (31% increase at 0.1 wt %)[172] reinforced with TRG. Ramanathan et al.[173] and Rafiee et al.[172] attributed this to the strong hydrogen-bonding interaction of oxygen-functionalized TRG and the mechanical interlocking at the wrinkled surface that may restrict segmental mobility of polymer chains near TRG surfaces. Still, the increase in PMMA modulus with only 0.01 wt % of TRG is unrealistically high. This enhancement even exceeds the Voigt upper bound prediction (the limit of perfect alignment and infinite particle aspect ratio A_f). To achieve the reported modulus, in addition to being perfectly aligned and infinitely long, the TRG sheets would need to increase the modulus of PMMA to 1 TPa for at least 5 nm on either side of each sheet.

Kim and co-workers[112] compared the stiffening performance of different types of functionalized graphene, dispersed via different blending routes in TPU elastomers. Despite different particle sizes, iGO and TRG gave nearly comparable tensile modulus increase (Table 4). This result indicates that stiffness increase is determined by the persistence length of the flexible graphene layers rather than A_f of fully extended sheets. For TRG composites, solvent processed (directly cast from the solution) composites have higher stiffness than melt processed ones. The lower modulus of melt processed composites may be due to reaggregation of particles under extensional flow during melt compounding. However, unlike the significant modulus gains for TPU (3- to 8-fold increase with 3 wt %), TRG only modestly improved the tensile stiffness for rigid glassy polymers PEN[125] and PC,[124] $<50\%$ increase at 3 wt %. Defects in the sheet structure formed by oxidation and pyrolysis possibly reduce the effective in-plane stiffness of TRG, which may account for the relatively small increase in tensile properties observed for glassy polymers.[125] Mori and Tanaka's micromechanical theory[174,175] was used to estimate the transverse tensile stiffness E_{11} of polymers (Poisson's ratio, $\nu = 0.4$) filled with perfectly aligned, 1 vol % $A_f = 200$ ellipsoids (e.g., graphene). These calculations are plotted in Figure 9 as a function of modulus ratio between pure reinforcement and matrix, $E_{ellipsoid}/E_{matrix}$. Reduction in graphene stiffness from 1000 GPa (modulus of defect-free) to 100 GPa diminishes modulus of rigid glassy polymers ($E_{matrix} = 3$ GPa) while it hardly affects that of elastomers ($E_{matrix} = 10$ MPa). These predictions also indicate that the composite stiffness cannot be improved further in the limit of extremely large stiffness contrast ($E_{ellipsoid}/E_{matrix} > 10^4$).

In addition to stiffness increase, improved tensile strength has been reported. Elongation to break typically decreases severely with the addition of rigid fillers. While elongation of most polymers decreased (negative signs in Table 4) with the addition of graphene, the decrease is less than one would expect, for example, for a similar amount of CB and certainly for the amount of CB needed to reach the same electrical conductivity. A nanoindentation study also revealed increased hardness of TRG reinforced PVA and PMMA.[114]

6.4. Thermocalorimetric Transitions. Significant increases in glass transition temperature T_g[116,122,173] and altered crystallization kinetics[143] of polymers by functionalized graphene dispersion have been observed. Ramanathan et al. report that TRG increased T_g of oxygen containing polymers such as PMMA (by 30 °C at 0.05 wt %) and poly(acrylonitrile) (PAN) (by 46 °C at 1 wt %) by hindering segmental motions of polymer chains via mechanical interlocking and hydrogen bonding with surface oxygen functionalities.[173] Whereas, for graphene oxide sheets esterified with PVA chains, PVA T_g elevation can be attributed to reduced chain mobility by covalent cross-linking.[122]

Graphene can nucleate crystallization of polymers. For polycaprolactone (PCL) and PVA, melt crystallization takes place at higher temperature and degree of crystallinity becomes greater after isothermal crystallization in the presence of graphene oxide[176,177] or TRG.[114,178] This is suggestive of strong interfacial interaction between polar polymer chains and functionalized graphene surface. TRG also induces new crystalline phases for poly(vinylidene fluoride) (PVDF).[143] Contradictory trends (suppressed crystallization by graphene addition) have also been reported. As a result of covalent grafting on GO, semicrystalline PVA[122] becomes completely amorphous.

6.5. Dimensional Stability. Graphite has a negative coefficient of thermal expansion (-1.5×10^{-6}/°C) in basal plane near room temperature.[179] Thermal expansion along the thickness direction is also far smaller (2.7×10^{-5}/°C)[180] than that of typical polymeric materials. Therefore, graphene can prevent dimensional changes of polymers when incorporated and oriented appropriately. Kalaitzidou et al. demonstrated GNP suppresses thermal expansion of PP as effectively as other carbon fillers such as CB and CNF, especially in the direction of platelet alignment.[151] Graphene oxide also reduced thermal expansion of epoxy (~30% reduction at 5 wt % incorporation).[117] However, Kim and Macosko found TRG is only marginally better or even less effective than graphite in improving dimensional stability of glassy polymers despite the higher aspect ratio.[124,125] They attributed this lower reinforcement efficiency of TRG to its wrinkled structure and flexibility.

6.6. Gas Permeation. Defect-free graphene sheets are impermeable to all gas molecules.[14] Combining graphene with polymeric hosts makes possible large scale barrier membranes with mechanical integrity, a significant advantage over 1-D SWCNT, MWCNT, or CNF. Kalaitzidou et al. reported GNP can reduce oxygen permeability more efficiently than 0-D (CB), 1-D (CNF), or even other 2-D fillers like organically modified montmorillonite (MMT) at similar loading.[151] Gas permeation data of graphene/polymer nanocomposites in the literature are summarized in Table 5. Kim and co-workers[112,124,125] compared gas permeation through polymeric membranes filled with different types of graphitic reinforcements. Figure 10 shows some of their results for TPU. Thermally or chemically treated GO layers decreased permeability of TPU more than organically modified MMT layers at similar loadings. Osman et al. reported a 25% decrease in oxygen permeation at 2.1 vol % MMT.[181] Especially, incorporation of iGO led to ~90% reduction in nitrogen permeability at 3 wt % loading, which theoretically can be attained by perfectly aligned, impermeable platelets with A_f of ~500 according to Lape and coworkers' model[182] for gas permeation of filled membranes. Also, solvent-based processing resulted in more reduction in permeation than the melt-based one, implying better dispersion of graphene platelets, in agreement with review of dispersion methods in section 5 and electrical and mechanical properties in sections 6.1 and 6.3.

6.7. Thermal Stability. Improved thermal stability of host polymers is another benefit expected from graphene-based reinforcements. Thermal degradation temperature, characterized by the maximum weight loss rate in thermogravimetry,

shifts up by 10−100 °C at <10 wt % graphene for PS,[51] PVA,[122,183] PMMA,[184] and silicone foams.[119] Decomposition of graphene composites is substantially slower than neat polymers, which is attributed to restricted chain mobility[51] of polymers near the graphene surface. During combustion, inflammable anisotropic nanoparticles form a jammed network of char layers that retards transport of the decomposition products.[185,186] This suggests application of graphene/polymer nanocomposites for flame retardation.

6.8. Synergy with Other Carbon Nanofillers. It is worth mentioning that a combination of carbon fillers with different dimensionality may lead to synergistic physical property gains for polymers. Epoxy resins containing a binary mixture of GNP and SWCNT in 3:1 weight ratio have higher thermal conductivity than ones reinforced with either individual filler.[158] Yu and colleagues explained this synergistic effect by bridging interactions between GNP and SWCNT that can reduce the interfacial resistance for thermal conduction. Also, mechanical properties such as hardness and stiffness of PVA can be enhanced more dramatically when graphene is dispersed with nanodiamonds.[178] 0-D nanodiamond particles at the interface may prevent clustering of graphene sheets.

7. Summary and Future Perspectives

7.1. Summary. Graphene is a multifunctional reinforcement that can improve electrical, thermal, mechanical, and gas barrier properties of polymers at extremely small loading. Graphene can provide a combination of the benefits achieved with layered silicates (gas permeation barrier and stiffness) and carbon nanotubes (electrical and thermal conductivity). These exfoliated carbon sheets can be produced via either bottom-up or top-down approaches. Bottom-up strategies, including CVD[15−21] and epitaxial growth from SiC,[24−30] produce large size graphene sheets with less defects, but in very limited quantity. Methods starting from chemically modified graphene precursors, particularly graphite oxide (GO), followed by chemical (CRG)[77−79] or thermal reduction (TRG)[89,90] are better suited for large scale production of reinforcements for the polymer composites.

Both CRG and TRG are electrically conductive but still have residual oxygen groups on the surface. These enable dispersion into solvents directly or with chemical functionalization[56] which then leads to facile blending with soluble polymers. Alternatively, composites can be processed by polymerizing monomers containing graphene. No studies yet have shown an advantage of in situ polymerization over solvent blending, and in some cases functional groups on the graphene may have interfered with the property improvements.[112] Melt compounding generally results in poorer dispersion but can be done more economically in large scale using melt extrusion. However, melt compounding is not an option for some chemically modified graphene materials which are prone to thermal degradation.

Dispersion of graphene in polymers can be characterized with TEM and by measuring solid properties. Linear viscoelastic measurements on composite melts[124,125] are also a useful tool to quantify dispersion. In the vicinity of particle percolation, nanocomposite melts start to develop a yield stress as well as a shear thinning behavior which can be probed by nonlinear viscoelastic tests.[129] As discussed earlier, dilute viscosity measurements can be also considered provided that graphene forms a stable dispersion.[96]

The onset concentration for electrical percolation is a good indicator for graphene dispersion since it is inversely proportional to the aspect ratio of randomly oriented disks. Graphene oriented parallel to the surface of polymer films can reduce gas permeation of polymeric membranes by as much as 90% at only 3 wt %.[112] Stiffness improvement by graphene is more pronounced for elastomers than glassy polymers due to the higher stiffness contrast between matrix and reinforcement. Extraordinarily high increase in modulus or glass transition temperature for PMMA, PAN, and epoxy by TRG[172,173] has been attributed to hydrogen-bonding interaction with oxygen-modified graphene surfaces, but we question some of these results in this Perspective.

7.2. Challenges. This versatility of graphene/polymer nanocomposites indicates their potential application in automotive, aerospace, electronics, and packaging. However, there are several challenges. The first is cost. Micromechanically produced mono- and bilayer graphene sheets are sold for 0.5−3 British pounds per μm^2 supported on SiO_2 substrate.[187] Although graphene can be derived more economically via GO, it will not see practical applications until commercial scale production of graphene is available at costs below CNT. Currently, the pricing of commercial, research grade CNT ranges from 1 to 2 USD/g (MWCNT)[188] to hundreds USD/g (SWCNT).[189] The average cost of GO estimated by the authors is 20−30 USD/kg, which is still higher than that of GNP (~10 USD/kg).[169] Moreover, GO synthesis produces acid wastes and the oxidation reaction involves potential risks for explosion. The thermal or chemical treatments required to exfoliate GO will add to the cost. There are currently two commercial sources for TRG: Vorbeck[190] and Angstron Materials.[191] Although there is no announced price for graphene, we estimate a target price of 50 USD/kg. Scale-up of graphene production (e.g., continuous fluidized bed reactor for TRG[92]) and recycling acid wastes would reduce the production cost of graphene materials.

Another barrier to practical use is difficult handling of graphene sheets in processing. Extremely low bulk density of high surface area graphene layers such as TRG makes processing into polymers in commercial scale challenging (e.g., difficult feeding into melt compounders). Densification for easy handling and transport may be necessary. Lightness of graphene sheets may also lead to human intake during handling. Biotoxicity of carbon nanomaterials including CNT to human has been frequently reported.[192,193] Prior to use, biocompatibility and safety of these 2-D nanocarbons must be tested, although their large lateral dimension and lack of entanglement make toxicity less likely than with CNT.

To date, the most commonly researched routes to graphene are via GO due to scalability. Even though these methods start from the same material, structure and surface characteristics may differ significantly depending on how the GO is exfoliated and reduced. Oxidation of graphite and thermal or chemical reduction lead to irreversible deformation of graphitic carbons, which can modify the micromechanical and electrical transport properties. However, mechanisms for defect formation and their influence on nanocomposite physical properties have not been fully understood yet. For instance, highly wrinkled structure and atomistic perforations in TRG may make the sheets less stiff and more permeable but may inhibit restacking. Moreover, there have been no direct comparisons of CRG and TRG for their dispersibility and interaction with polymers. Synthetic routes to graphene layers avoiding the structural deformation or unnecessary functionalization and post-treatments that can restore graphitic planar domains need to be sought to maximize property increase for polymeric materials. For instance, thermal curing is reported to increase carbon to oxygen ratio in TRG.[61,92,194] More use of molecular modeling will help to guide experimental strategies.[57,59,74,195,196]

Even at the same loading, nanocomposite properties strongly depend on spatial distribution of the anisotropic inclusions. As a result of high shear or elongational flow fields, melt processing tends to yield highly aligned morphology of platelet-like fillers than solvent mixing.[112] Morphology and properties of the composites are sensitive to post-shaping such as stretching or injection molding which induces orientation and migration of particles.[124,197−199] The influence of shear deformation on viscosity and electrical conductivity of CNT/polymer melts has been extensively studied.[200,201] These properties are based on particle connectivity and thus generally benefit from random orientation of anisotropic inclusions.[135,202] On the other hand, particle orientation typically improves mechanical and gas permeation properties.[203,204] Since no single composite morphology will attain all desired properties simultaneously, it is important to engineer the spatial arrangement of dispersed nanoparticles appropriately for target properties. Current strategies and challenges to control composite morphology are well discussed in the review by Vaia and Maguire.[205]

Adhesion between graphene and polymers is also an important factor to be considered in designing composite materials. Superior mechanics of carbon nanofillers can be fully realized when they are strongly bonded to matrix polymers.[206,207] Improved adhesion may prevent interfacial scattering of phonons and yield higher composite thermal conductivity as well as minimize interfacial free volume which affects gas permeation. Shenogina et al. found interfacial thermal conductance can be correlated with the wetting properties.[164] Covalently attaching alkyl chains on graphene edges can improve thermal conduction across the graphene/hydrocarbon interface.[208] TRG appears to bind strongly with some oxygen containing polymers as substantiated by highly enhanced stiffness and T_g of the matrix.[172,173] However, such an appreciable T_g increase was never observed by us for PC and PEN.

7.3. Future Application. As reviewed in section 6.7, the excellent thermal stability of graphene-based nanocomposites can be used for producing flame-retardant materials. Networks of CNT,[185] CNF,[209] and EG[210] are known to retard flammability of PMMA and also PU foams. Its aromatic and 2-D nature makes graphene an ideal alternative for the flame-retarding additives. Also, high electrical or thermal conductivity of graphene/polymer nanocomposites may satisfy conditions for heat- or electricity-activated shape memory,[113,211] static charge dissipation, and electromagnetic wave reflective materials.[148,212] Especially near the percolation threshold, resistivity of composites can vary dramatically upon temperature change,[213] solvent attack,[214] and external strain.[215] This on−off phenomena in electrical conductivity[148] by external stimuli can be used for electrical switching and strain/solvent sensing. Graphene nanocomposites have potential as photo- or electromechanical actuators since mechanical response has been induced by infrared radiation[216] or electric potential[217] in CNT composites.

The transmittance of visible light is attenuated by ~2.3% as it penetrates through a single layer of graphene.[218] If thin layers of electrically conductive graphene can be deposited on glass or polymer surfaces, flexible displays,[219] thin-film transistors,[220] and photovoltaic[221] and liquid crystal devices[222] will be made possible. TRG conductive inks are already being offered commercially.[149] Recently, homogeneous coating of a few-layer-thick graphene has been demonstrated via direct transfer of graphene films from CVD metal substrates[219] or from vacuum filtration membranes[220] as well as by conventional spin-coating.[221,223]

Acknowledgment. Financial support from the Abu Dhabi-Minnesota Institute for Research Excellence (ADMIRE), a partnership between the Petroleum Institute of Abu Dhabi and the Department of Chemical Engineering and Materials Science of the University of Minnesota, is acknowledged. The authors also appreciate helpful input from Prof. K. Andre Mkhoyan at the University of Minnesota and Prof. Matteo Pasquali and Natnael Behabtu at Rice University.

References and Notes

(1) Huang, J.-C. *Adv. Polym. Technol.* **2002**, *21*, 299–313.
(2) Moniruzzaman, M.; Winey, K. I. *Macromolecules* **2006**, *39*, 5194–5205.
(3) Okamoto, M. *Polymer/Clay Nanocomposites*; American Scientific Publishers: Stevenson Ranch, CA, 2004; Vol. *8*.
(4) Geim, A. K.; Novoselov, K. S. *Nature Mater.* **2007**, *6*, 183–191.
(5) Lax, A.; Maxwell, R. *Natl. Trust Ann. Archaeol. Rev.* **1998−1999**, 18–23.
(6) Weinberg, S. S. *The Stone Age in the Agean*, 10th ed.; Cambridge University Press: Cambridge, 2007; Vol. *1*.
(7) Iijima, S. *Nature* **1991**, *354*, 56–58.
(8) Kroto, H. W.; Heath, J. R.; O'Brien, S. C.; Curl, R. F.; Smalley, R. E. *Nature* **1985**, *318*, 162–163.
(9) Eizenberg, M.; Blakely, J. M. *Surf. Sci.* **1970**, *82*, 228–236.
(10) Novoselov, K. S.; Geim, A. K.; Morozov, S. V.; Jiang, D.; Zhang, Y.; Dubonos, S. V.; Grigorieva, I. V.; Firsov, A. A. *Science* **2004**, *306*, 666–669.
(11) Lee, C.; Wei, X.; Kysar, J. W.; Hone, J. *Science* **2008**, *321*, 385–388.
(12) Balandin, A. A.; Ghosh, S.; Bao, W.; Calizo, I.; Teweldebrhan, D.; Miao, F.; Lau, C. N. *Nano Lett.* **2008**, *8*, 902–907.
(13) Du, X.; Skachko, I.; Barker, A.; Andrei, E. Y. *Nature Nanotechnol.* **2008**, *3*, 491–495.
(14) Bunch, J. S.; Verbridge, S. S.; Alden, J. S.; van der Zande, A. M.; Parpia, J. M.; Craighead, H. G.; McEuen, P. L. *Nano Lett.* **2008**, *8*, 2458–2462.
(15) Wang, X.; You, H.; Liu, F.; Li, M.; Wan, L.; Li, S.; Li, Q.; Xu, Y.; Tian, R.; Yu, Z.; Xiang, D.; Cheng, J. *Chem. Vapor Deposition* **2009**, *15*, 53–56.
(16) Wang, Y.; Chen, X.; Zhong, Y.; Zhu, F.; Loh, K. P. *Appl. Phys. Lett.* **2009**, *95*, 063302/1–063302/3.
(17) Xianbao, W.; Haijun, Y.; Fangming, L.; Mingjian, L.; Li, W.; Shaoqing, L.; Qin, L.; Yang, X.; Rong, T.; Ziyong, Y.; Dong, X.; Jing, C. *Chem. Vapor Deposition* **2009**, *15*, 53–56.
(18) Dervishi, E.; Li, Z.; Watanabe, F.; Biswas, A.; Xu, Y.; Biris Alexandru, R.; Saini, V.; Biris Alexandru, S. *Chem. Commun.* **2009**, 4061–4063.
(19) Li, X.; Cai, W.; An, J.; Kim, S.; Nah, J.; Yang, D.; Piner, R.; Velamakanni, A.; Jung, I.; Tutuc, E.; Banerjee, S. K.; Colombo, L.; Ruoff, R., S. *Science* **2009**, *324*, 1312–1314.
(20) Chong-an, D.; Dacheng, W.; Gui, Y.; Yunqi, L.; Yunlong, G.; Daoben, Z. *Adv. Mater.* **2008**, *20*, 3289–3293.
(21) Chae, S. J.; Günes, F.; Kim, K. K.; Kim, E. S.; Han, G. H.; Kim, S. M.; Shin, H.-J.; Yoon, S.-M.; Choi, J.-Y.; Park, M. H.; Yang, C. W.; Pribat, D.; Lee, Y. H. *Adv. Mater.* **2009**, *21*, 2328–2333.
(22) Li, N.; Wang, Z.; Zhao, K.; Shi, Z.; Gu, Z.; Xu, S. *Carbon* **2009**, *48*, 255–259.
(23) Karmakar, S.; Kulkarni, N. V.; Nawale, A. B.; Lalla, N. P.; Mishra, R.; Sathe, V. G.; Bhoraskar, S. V.; Das, A. K. *J. Phys. D: Appl. Phys.* **2009**, *42*, 115201/1–115201/14.
(24) Rollings, E.; Gweon, G.-H.; Zhou, S. Y.; Mun, B. S.; McChesney, J. L.; Hussain, B. S.; Fedorov, A. V.; First, P. N.; de Heer, W. A.; Lanzar, A. *J. Phys. Chem. Solids* **2006**, *67*, 2172–2177.
(25) de Heer, W. A.; Berger, C.; Wu, X.; First, P. N.; Conrad, E. H.; Li, X.; Li, T.; Sprinkle, M.; Hass, J.; Sadowski, M. L.; Potemski, M.; Martinez, G. *Solid State Commun.* **2007**, *143*, 92–100.
(26) Alexander, M.; Oleg, P. *Phys. Status Solidi B* **2008**, *245*, 1425–1435.
(27) Ni, Z. H.; Chen, W.; Fan, X. F.; Kuo, J. L.; Yu, T.; Wee, A. T. S.; Shen, Z. X. *Phys. Rev. B: Condens. Matter* **2008**, *77*, 115416/1–115416/6.
(28) Sutter, P. W.; Flege, J.-I.; Sutter, E. A. *Nature Mater.* **2008**, *7*, 406–411.
(29) Seyller, T.; Bostwick, A.; Emtsev, K. V.; Horn, K.; Ley, L.; McChesney, J. L.; Ohta, T.; Riley, J. D.; Rotenberg, E.; Speck, F. *Phys. Status Solidi B* **2008**, *245*, 1436–1446.

(30) Sprinkle, M.; Soukiassian, P.; de Heer, W. A.; Berger, C.; Conrad, E. H. *Phys. Status Solidi RRL* **2009**, *3*, A91–A94.
(31) Yannick, C.; Wim, K. *ChemPhysChem* **2006**, *7*, 1770–1778.
(32) Yang, X.; Dou, X.; Rouhanipour, A.; Zhi, L.; Rader Hans, J.; Mullen, K. *J. Am. Chem. Soc.* **2008**, *130*, 4216–7.
(33) Zhi, L.; Muellen, K. *J. Mater. Chem.* **2008**, *18*, 1472–1484.
(34) Kim, C.-D.; Min, B.-K.; Jung, W.-S. *Carbon* **2009**, *47*, 1610–1612.
(35) Kosynkin, D. V.; Higginbotham, A. L.; Sinitskii, A.; Lomeda, J. R.; Dimiev, A.; Price, B. K.; Tour, J. M. *Nature* **2009**, *458*, 872–876.
(36) Hirsch, A. *Angew. Chem., Int. Ed.* **2009**, *48*, 6594–6596.
(37) Jiao, L.; Zhang, L.; Wang, X.; Diankov, G.; Dai, H. *Nature* **2009**, *458*, 877–880.
(38) Zhang, W.; Cui, J.; Tao, C.-a.; Wu, Y.; Li, Z.; Ma, L.; Wen, Y.; Li, G. *Angew. Chem., Int. Ed.* **2009**, *48*, 5864–5868.
(39) Worsley, K. A.; Ramesh, P.; Mandal, S. K.; Niyogi, S.; Itkis, M. E.; Haddon, R. C. *Chem. Phys. Lett.* **2007**, *445*, 51–56.
(40) Kelly, T. D.; Matos, G. R. In Historical Statistics for Mineral and Material Commodities in the United States, U.S. Geological Survey Data Series 140, **2010**.
(41) Viculis, L. M.; Mack, J. J.; Mayer, O. M.; Hahn, H. T.; Kaner, R. B. *J. Mater. Chem.* **2005**, *15*, 974–978.
(42) Carr, K. E. *Carbon* **1970**, *8*, 155–166.
(43) Chen, G.; Wu, D.; Weng, W.; Wu, C. *Carbon* **2003**, *41*, 619–621.
(44) Celzard, A.; Mareche, J. F.; Furdin, G. *Carbon* **2002**, *40*, 2713–2718.
(45) Lee, J. H.; Shin, D. W.; Makotchenko, V. G.; Nazarov, A. S.; Fedorov, V. E.; Kim, Y. H.; Choi, J.-Y.; Kim, J. M.; Yoo, J.-B. *Adv. Mater.* **2009**, *21*, 4383–4387.
(46) Fukushima, H. Ph.D. Thesis, Michigan State University, 2003.
(47) Kalaitzidou, K.; Fukushima, H.; Drzal, L. T. *Compos. Sci. Technol.* **2007**, *67*, 2045–2051.
(48) Kalaitzidou, K.; Fukushima, H.; Askeland, P.; Drzal, L. T. *J. Mater. Sci.* **2008**, *43*, 2895–2907.
(49) Bourlinos, A. B.; Georgakilas, V.; Zboril, R.; Steriotis, T. A.; Stubos, A. *Small* **2009**, *5*, 1841–1845.
(50) Hernandez, Y.; Nicolosi, V.; Lotya, M.; Blighe, F. M.; Sun, Z.; De, S.; McGovern, I. T.; Holland, B.; Byrne, M.; Gun'Ko, Y. K.; Boland, J. J.; Niraj, P.; Duesberg, G.; Krishnamurthy, S.; Goodhue, R.; Hutchison, J.; Scardaci, V.; Ferrari, A. C.; Coleman, J. N. *Nature Nanotechnol.* **2008**, *3*, 563–568.
(51) Liu, N.; Luo, F.; Wu, H.; Liu, Y.; Zhang, C.; Chen, J. *Adv. Funct. Mater.* **2008**, *18*, 1518–1525.
(52) Behabtu, N.; Lomeda, J. R.; Green, M. J.; Higginbotham, A. L.; Sinitskii, A.; Kosynkin, D. V.; Tsentalovich, D.; Parra-Vasquez, A. N. G.; Schmidt, J.; Kesselman, E.; Cohen, Y.; Talmon, Y.; Tour, J. M.; Pasquali, M. *Nature Nanotechnol.* **2010**, *5*, 406–411.
(53) Brodie, B. C. *Philos. Trans. R. Soc. London* **1859**, *149*, 249–259.
(54) Staudenmaier, L. *Ber. Dtsch. Chem. Ges.* **1898**, *31*, 1481–87.
(55) Hummers, W. S., Jr.; Offeman, R. E. *J. Am. Chem. Soc.* **1958**, *80*, 1339.
(56) Park, S.; Ruoff, R. S. *Nature Nanotechnol.* **2009**, *4*, 217–224.
(57) Boukhvalov, D. W.; Katsnelson, M. I. *J. Am. Chem. Soc.* **2008**, *130*, 10697–10701.
(58) Lahaye, R. J. W. E.; Jeong, H. K.; Park, C. Y.; Lee, Y. H. *Phys. Rev. B: Condens. Matter* **2009**, *79*, 125435/1–125435/8.
(59) Paci, J. T.; Belytschko, T.; Schatz, G. C. *J. Phys. Chem. C* **2007**, *111*, 18099–18111.
(60) Zhang, W. H.; Carravetta, V.; Li, Z. Y.; Luo, Y.; Yang, J. L. *J. Chem. Phys.* **2009**, *131*, 244505/1–244505/6.
(61) Gao, W.; Alemany, L. B.; Ci, L.; Ajayan, P. M. *Nature Chem.* **2009**, *1*, 403−408, S403/1−S403/20.
(62) Jeong, H.-K.; Lee, Y. P.; Lahaye, R. J. W. E.; Park, M.-H.; An, K. H.; Kim, I. J.; Yang, C.-W.; Park, C. Y.; Ruoff, R. S.; Lee, Y. H. *J. Am. Chem. Soc.* **2008**, *130*, 1362–1366.
(63) Cai, W.; Piner, R. D.; Stadermann, F. J.; Park, S.; Shaibat, M. A.; Ishii, Y.; Yang, D.; Velamakanni, A.; An, S. J.; Stoller, M.; An, J.; Chen, D.; Ruoff, R. S. *Science* **2008**, *321*, 1815–1817.
(64) Szabo, T.; Berkesi, O.; Forgo, P.; Josepovits, K.; Sanakis, Y.; Petridis, D.; Dekany, I. *Chem. Mater.* **2006**, *18*, 2740–2749.
(65) Hristea, G.; Panaitescu, C. *Rev. Roum. Chim.* **2002**, *46*, 1107–1111.
(66) Lerf, A.; He, H.; Forster, M.; Klinowski, J. *J. Phys. Chem. B* **1998**, *102*, 4477–4482.
(67) He, H.; Klinowski, J.; Forster, M.; Lerf, A. *Chem. Phys. Lett.* **1998**, *287*, 53–56.
(68) Mermoux, M.; Chabre, Y.; Rousseau, A. *Carbon* **1991**, *29*, 469–74.
(69) Nakajima, T.; Mabuchi, A.; Hagiwara, R. *Carbon* **1988**, *26*, 357–61.
(70) Scholz, W.; Boehm, H. P. *Z. Anorg. Allg. Chem.* **1969**, *369*, 327–40.
(71) Clauss, A.; Plass, R.; Boehm, H. P.; Hofmann, U. *Z. Anorg. Allg. Chem.* **1957**, *291*, 205–20.
(72) Mkhoyan, K. A.; Contryman, A. W.; Silcox, J.; Stewart, D. A.; Eda, G.; Mattevi, C.; Miller, S.; Chhowalla, M. *Nano Lett.* **2009**, *9*, 1058–1063.
(73) Herrera-Alonso, M.; Abdala, A. A.; McAllister, M. J.; Aksay, I. A.; Prud'homme, R. K. *Langmuir* **2007**, *23*, 10644–10649.
(74) Li, J.-L.; Kudin, K. N.; McAllister, M. J.; Prud'homme, R. K.; Aksay, I. A.; Car, R. *Phys. Rev. Lett.* **2006**, *96*, 176101/1–176101/4.
(75) Dreyer, D. R.; Park, S.; Bielawski, C. W.; Ruoff, R. S. *Chem. Soc. Rev.* **2010**, *39*, 228–240.
(76) Stankovich, S.; Piner, R. D.; Chen, X.; Wu, N.; Nguyen, S. T.; Ruoff, R. S. *J. Mater. Chem.* **2006**, *16*, 155–158.
(77) Stankovich, S.; Dikin, D. A.; Piner, R. D.; Kohlhaas, K. A.; Kleinhammes, A.; Jia, Y.; Wu, Y.; Nguyen, S. T.; Ruoff, R. S. *Carbon* **2007**, *45*, 1558–1565.
(78) Wang, G.; Shen, X.; Wang, B.; Yao, J.; Park, J. *Carbon* **2009**, *47*, 1359–1364.
(79) Lomeda, J. R.; Doyle, C. D.; Kosynkin, D. V.; Hwang, W.-F.; Tour, J. M. *J. Am. Chem. Soc.* **2008**, *130*, 16201–16206.
(80) Wang, H.; Robinson, J. T.; Li, X.; Dai, H. *J. Am. Chem. Soc.* **2009**, *131*, 9910–9911.
(81) Stankovich, S.; Dikin, D. A.; Dommett, G. H. B.; Kohlhaas, K. M.; Zimney, E. J.; Stach, E. A.; Piner, R. D.; Nguyen, S. T.; Ruoff, R. S. *Nature* **2006**, *442*, 282–286.
(82) Si, Y.; Samulski, E. T. *Nano Lett.* **2008**, *8*, 1679–1682.
(83) Wang, G.; Yang, J.; Park, J.; Gou, X.; Wang, B.; Liu, H.; Yao, J. *J. Phys. Chem. C* **2008**, *112*, 8192–8195.
(84) Williams, G.; Seger, B.; Kamat, P. V. *ACS Nano* **2008**, *2*, 1487–1491.
(85) Zhou, Y.; Bao, Q.; Tang, L. A. L.; Zhong, Y.; Loh, K. P. *Chem. Mater.* **2009**, *21*, 2950–2956.
(86) Nethravathi, C.; Rajamathi, M. *Carbon* **2008**, *46*, 1994–1998.
(87) Fan, Z.; Wang, K.; Wei, T.; Yan, J.; Song, L.; Shao, B. *Carbon* **2010**, *48*, 1670–1692.
(88) Prud'homme, R. K.; Aksay, I. A.; Adamson, D.; Abdala, A. U.S. Patent 20070092432, 2007.
(89) Schniepp, H. C.; Li, J.-L.; McAllister, M. J.; Sai, H.; Herrera-Alonso, M.; Adamson, D. H.; Prud'homme, R. K.; Car, R.; Saville, D. A.; Aksay, I. A. *J. Phys. Chem. B* **2006**, *110*, 8535–8539.
(90) McAllister, M. J.; Li, J.-L.; Adamson, D. H.; Schniepp, H. C.; Abdala, A. A.; Liu, J.; Herrera-Alonso, M.; Milius, D. L.; Car, R.; Prud'homme, R. K.; Aksay, I. A. *Chem. Mater.* **2007**, *19*, 4396–4404.
(91) Steurer, P.; Wissert, R.; Thomann, R.; Muelhaupt, R. *Macromol. Rapid Commun.* **2009**, *30*, 316–327.
(92) Aksay, I. A.; Milius, D. L.; Korkut, S.; Prud'homme, R. K. W.O. Patent 2009/134492 A2, 2009.
(93) Schniepp, H. C.; Kudin, K. N.; Li, J.-L.; Prud'homme, R. K.; Car, R.; Saville, D. A.; Aksay, I. A. *ACS Nano* **2008**, *2*, 2577–2584.
(94) Stankovich, S.; Piner, R. D.; Nguyen, S. T.; Ruoff, R. S. *Carbon* **2006**, *44*, 3342–3347.
(95) Meyer, J. C.; Geim, A. K.; Katsnelson, M. I.; Novoselov, K. S.; Obergfell, D.; Roth, S.; Girit, C.; Zettl, A. *Solid State Commun.* **2007**, *143*, 101–109.
(96) Parra-Vasquez, A. N. G.; Stepanek, I.; Davis, V. A.; Moore, V. C.; Haroz, E. H.; Shaver, J.; Hauge, R. H.; Smalley, R. E.; Pasquali, M. *Macromolecules* **2007**, *40*, 4043–4047.
(97) Spector, M. S.; Naranjo, E.; Chiruvolu, S.; Zasadzinski, J. A. *Phys. Rev. Lett.* **1994**, *73*, 2867–70.
(98) Wen, X.; Garland, C. W.; Hwa, T.; Kardar, M.; Kokufuta, E.; Li, Y.; Orkisz, M.; Tanaka, T. *Nature* **1992**, *355*, 426–428.
(99) Shin, H.-J.; Kim, K. K.; Benayad, A.; Yoon, S.-M.; Park, H. K.; Jung, I.-S.; Jin, M. H.; Jeong, H.-K.; Kim, J. M.; Choi, J.-Y.; Lee, Y. H. *Adv. Funct. Mater.* **2009**, *19*, 1987–1992.
(100) Hontoria-Lucas, C.; Lopez-Peinado, A. J.; Lopez-Gonzalez, J. d. D.; Rojas-Cervantes, M. L.; Martin-Aranda, R. M. *Carbon* **1995**, *33*, 1585–1592.
(101) Szabo, T.; Berkesi, O.; Dekany, I. *Carbon* **2005**, *43*, 3186–3189.
(102) Titelman, G. I.; Gelman, V.; Bron, S.; Khalfin, R. L.; Cohen, Y.; Bianco-Peled, H. *Carbon* **2005**, *43*, 641–649.
(103) Kudin, K. N.; Ozbas, B.; Schniepp, H. C.; Prud'homme, R. K.; Aksay, I. A.; Car, R. *Nano Lett.* **2008**, *8*, 36–41.

(104) Cancado, L. G.; Takai, K.; Enoki, T.; Endo, M.; Kim, Y. A.; Mizusaki, H.; Speziali, N. L.; Jorio, A.; Pimenta, M. A. *Carbon* **2008**, *46*, 272–275.
(105) Jung, I.; Dikin, D.; Park, S.; Cai, W.; Mielke, S. L.; Ruoff, R. S. *J. Phys. Chem. C* **2008**, *112*, 20264–20268.
(106) Jung, I.; Dikin, D. A.; Piner, R. D.; Ruoff, R. S. *Nano Lett.* **2008**, *8*, 4283–4287.
(107) Mickelson, E. T.; Huffman, C. B.; Rinzler, A. G.; Smalley, R. E.; Hauge, R. H.; Margrave, J. L. *Chem. Phys. Lett.* **1998**, *296*, 188–194.
(108) Chen, J.; Hamon, M. A.; Hu, H.; Chen, Y.; Rao, A. M.; Eklund, P. C.; Haddon, R. C. *Science* **1998**, *282*, 95–98.
(109) Bahr, J. L.; Yang, J.; Kosynkin, D. V.; Bronikowski, M. J.; Smalley, R. E.; Tour, J. M. *J. Am. Chem. Soc.* **2001**, *123*, 6536–6542.
(110) Matsuo, Y.; Tahara, K.; Sugie, Y. *Carbon* **1997**, *35*, 113–120.
(111) Hirata, M.; Gotou, T.; Horiuchi, S.; Fujiwara, M.; Ohba, M. *Carbon* **2004**, *42*, 2929–2937.
(112) Kim, H.; Miura, Y.; Macosko, C. W. *Chem. Mater.* **2010**, *22*, 3441–3450.
(113) Liang, J.; Xu, Y.; Huang, Y.; Zhang, L.; Wang, Y.; Ma, Y.; Li, F.; Guo, T.; Chen, Y. *J. Phys. Chem. C* **2009**, *113*, 9921–9927.
(114) Das, B.; Prasad, K. E.; Ramamurty, U.; Rao, C. N. R. *Nanotechnology* **2009**, *20*, 125705/1–125705/5.
(115) Liu, P.; Gong, K.; Xiao, P.; Xiao, M. *J. Mater. Chem.* **2000**, *10*, 933–935.
(116) Jang, J. Y.; Kim, M. S.; Jeong, H. M.; Shin, C. M. *Compos. Sci. Technol.* **2009**, *69*, 186–191.
(117) Wang, S.; Tambraparni, M.; Qiu, J.; Tipton, J.; Dean, D. *Macromolecules* **2009**, *42*, 5251–5255.
(118) Du, X. S.; Xiao, M.; Meng, Y. Z.; Hay, A. S. *Carbon* **2005**, *43*, 195–213.
(119) Verdejo, R.; Barroso-Bujans, F.; Angel Rodriguez-Perez, M.; de Saja, J. A.; Angel Lopez-Manchado, M. *J. Mater. Chem.* **2008**, *18*, 2221–2226.
(120) Lee, Y. R.; Raghu, A. V.; Jeong, H. M.; Kim, B. K. *Macromol. Chem. Phys.* **2009**, *210*, 1247–1254.
(121) Yang, Y.; Wang, J.; Zhang, J.; Liu, J.; Yang, X.; Zhao, H. *Langmuir* **2009**, *25*, 11808–11814.
(122) Salavagione, H. J.; Gomez, M. A.; Martinez, G. *Macromolecules* **2009**, *42*, 6331–6334.
(123) Prud'homme, R. K.; Ozbas, B.; Aksay, I. A.; Register, R. A.; Adamson, D. H. W.O. Patent 2008045778 A1, 2008.
(124) Kim, H.; Macosko, C. W. *Polymer* **2009**, *50*, 3797–3809.
(125) Kim, H.; Macosko, C. W. *Macromolecules* **2008**, *41*, 3317–3327.
(126) Wakabayashi, K.; Pierre, C.; Dikin, D. A.; Ruoff, R. S.; Ramanathan, T.; Brinson, L. C.; Torkelson, J. M. *Macromolecules* **2008**, *41*, 1905–1908.
(127) Drummy, L. F.; Wang, Y. C.; Schoenmakers, R.; May, K.; Jackson, M.; Koerner, H.; Farmer, B. L.; Mauryama, B.; Vaia, R. A. *Macromolecules* **2008**, *41*, 2135–2143.
(128) Fornes, T. D.; Paul, D. R. *Polymer* **2003**, *44*, 4993–5013.
(129) Vermant, J.; Ceccia, S.; Dolgovskij, M. K.; Maffettone, P. L.; Macosko, C. W. *J. Rheol.* **2007**, *51*, 429–450.
(130) Zosel, A. *Rheol. Acta* **1982**, *21*, 72–80.
(131) Garboczi, E. J.; Snyder, K. A.; Douglas, J. F.; Thorpe, M. F. *Phys. Rev. E* **1995**, *52*, 819–28.
(132) Celzard, A.; McRae, E.; Deleuze, C.; Dufort, M.; Furdin, G.; Mareche, J. F. *Phys. Rev. B: Condens. Matter* **1996**, *53*, 6209–14.
(133) Ren, J.; Silva, A. S.; Krishnamoorti, R. *Macromolecules* **2000**, *33*, 3739–3746.
(134) Shante, V. K. S.; Kirkpatrick, S. *Adv. Phys.* **1971**, *20*, 325.
(135) Du, F.; Scogna, R. C.; Zhou, W.; Brand, S.; Fischer, J. E.; Winey, K. I. *Macromolecules* **2004**, *37*, 9048–9055.
(136) Krishnamoorti, R.; Giannelis, E. P. *Macromolecules* **1997**, *30*, 4097–4102.
(137) Ren, J.; Casanueva, B. F.; Mitchell, C. A.; Krishnamoorti, R. *Macromolecules* **2003**, *36*, 4188–4194.
(138) Alig, I.; Skipa, T.; Lellinger, D.; Poetschke, P. *Polymer* **2008**, *49*, 3524–3532.
(139) Cipriano, B. H.; Kota, A. K.; Gershon, A. L.; Laskowski, C. J.; Kashiwagi, T.; Bruck, H. A.; Raghavan, S. R. *Polymer* **2008**, *49*, 4846–4851.
(140) Munson-McGee, S. H. *Phys. Rev. B* **1991**, *43*, 3331–3336.
(141) Balberg, I.; Binenbaum, N.; Wagner, N. *Phys. Rev. Lett.* **1984**, *52*, 1465–1468.
(142) Wei, T.; Luo, G.; Fan, Z.; Zheng, C.; Yan, J.; Yao, C.; Li, W.; Zhang, C. *Carbon* **2009**, *47*, 2296–2299.
(143) Ansari, S.; Giannelis, E. P. *J. Polym. Sci., Part B: Polym. Phys.* **2009**, *47*, 888–897.
(144) Wang, W.-P.; Pan, C.-Y. *Polym. Eng. Sci.* **2004**, *44*, 2335–2339.
(145) Raghu, A. V.; Lee, Y. R.; Jeong, H. M.; Shin, C. M. *Macromol. Chem. Phys.* **2008**, *209*, 2487–2493.
(146) Nguyen, D. A.; Lee, Y. R.; Raghu, A. V.; Jeong, H. M.; Shin, C. M.; Kim, B. K. *Polym. Int.* **2009**, *58*, 412–417.
(147) Liang, J.; Wang, Y.; Huang, Y.; Ma, Y.; Liu, Z.; Cai, J.; Zhang, C.; Gao, H.; Chen, Y. *Carbon* **2009**, *47*, 922–925.
(148) Chung, D. D. L. *J. Mater. Sci.* **2004**, *39*, 2645–2661.
(149) Lettow, J. S.; Aksay, I. A.; Korkut, S.; Chiang, K. S. U.S. Patent 20070092432 A1, 2009.
(150) Brandrup, J.; Immergut, E. H.; Grulke, E. A.; Abe, A.; Bloch, D. R. *Polymer Handbook*, 4th ed.; John Wiley & Sons: New York, 2005.
(151) Kalaitzidou, K.; Fukushima, H.; Drzal, L. T. *Carbon* **2007**, *45*, 1446–1452.
(152) Kim, S.; Do, I.; Drzal, L. T. *Macromol. Mater. Eng.* **2009**, *294*, 196–205.
(153) Prasher, R. S.; Chang, J.-Y.; Sauciuc, I.; Narasimhan, S.; Chau, D.; G., C.; Myers, A.; Prstic, S.; Hu, C. *Intel Tech. J.* **2005**, *9*, 285–296.
(154) Biercuk, M. J.; Llaguno, M. C.; Radosavljevic, M.; Hyun, J. K.; Johnson, A. T.; Fischer, J. E. *Appl. Phys. Lett.* **2002**, *80*, 2767–2769.
(155) Leong, C.-K.; Chung, D. D. L. *Carbon* **2003**, *41*, 2459–2469.
(156) Xie, S. H.; Liu, Y. Y.; Li, J. Y. *Appl. Phys. Lett.* **2008**, *92*, 243121/1–243121/3.
(157) Ghose, S.; Working, D. C.; Connell, J. W.; Smith, J. G., Jr.; Watson, K. A.; Delozier, D. M.; Sun, Y. P.; Lin, Y. *High Perform. Polym.* **2006**, *18*, 961–977.
(158) Yu, A.; Ramesh, P.; Sun, X.; Bekyarova, E.; Itkis, M. E.; Haddon, R. C. *Adv. Mater.* **2008**, *20*, 4740–4744.
(159) Yu, A.; Ramesh, P.; Itkis, M. E.; Bekyarova, E.; Haddon, R. C. *J. Phys. Chem. C* **2007**, *111*, 7565–7569.
(160) Huxtable, S. T.; Cahill, D. G.; Shenogin, S.; Xue, L.; Ozisik, R.; Barone, P.; Usrey, M.; Strano, M. S.; Siddons, G.; Shim, M.; Keblinski, P. *Nature Mater.* **2003**, *2*, 731–734.
(161) Kim, P.; Shi, L.; Majumdar, A.; McEuen, P. L. *Phys. Rev. Lett.* **2001**, *87*, 215502/1–215502/4.
(162) Zhong, H.; Lukes, J. R. *Phys. Rev. B: Condens. Matter* **2006**, *74*, 125403/1–125403/10.
(163) Pollack, G. L. *Rev. Mod. Phys.* **1969**, *41*, 48–81.
(164) Shenogina, N.; Godawat, R.; Keblinski, P.; Garde, S. *Phys. Rev. Lett.* **2009**, *102*, 156101/1–156101/4.
(165) Shenogin, S.; Bodapati, A.; Xue, L.; Ozisik, R.; Keblinski, P. *Appl. Phys. Lett.* **2004**, *85*, 2229–2231.
(166) Liu, C. H.; Fan, S. S. *Appl. Phys. Lett.* **2005**, *86*, 123106/1–123106/3.
(167) Veca, L. M.; Meziani, M. J.; Wang, W.; Wang, X.; Lu, F.; Zhang, P.; Lin, Y.; Fee, R.; Connell, J. W.; Sun, Y.-P. *Adv. Mater.* **2009**, *21*, 2088–2092.
(168) Ganguli, S.; Roy, A. K.; Anderson, D. P. *Carbon* **2008**, *46*, 806–817.
(169) Fukushima, H.; Drzal, L. T.; Rook, B. P.; Rich, M. J. *J. Therm. Anal. Calorim.* **2006**, *85*, 235–238.
(170) Kim, S.; Drzal, L. T. *Sol. Energy Mater.* **2009**, *93*, 136–142.
(171) Gomez-Navarro, C.; Burghard, M.; Kern, K. *Nano Lett.* **2008**, *8*, 2045–2049.
(172) Rafiee, M. A.; Rafiee, J.; Wang, Z.; Song, H.; Yu, Z.-Z.; Koratkar, N. *ACS Nano* **2009**, *3*, 3884–3890.
(173) Ramanathan, T.; Abdala, A. A.; Stankovich, S.; Dikin, D. A.; Herrera-Alonso, M.; Piner, R. D.; Adamson, D. H.; Schniepp, H. C.; Chen, X.; Ruoff, R. S.; Nguyen, S. T.; Aksay, I. A.; Prud'Homme, R. K.; Brinson, L. C. *Nature Nanotechnol.* **2008**, *3*, 327–331.
(174) Mori, T.; Tanaka, K. *Acta Metall.* **1973**, *21*, 571–574.
(175) Tandon, G. P.; Weng, G. J. *Polym. Compos.* **1984**, *5*, 327–333.
(176) Kai, W.; Hirota, Y.; Hua, L.; Inoue, Y. *J. Appl. Polym. Sci.* **2008**, *107*, 1395–1400.
(177) Cai, D.; Song, M. *Nanotechnology* **2009**, *20*, 315708/1–315708/6.
(178) Prasad, K. E.; Das, B.; Maitra, U.; Ramamurty, U.; Rao, C. N. R. *Proc. Natl. Acad. Sci. U.S.A.* **2009**, *106*, 13186−13189, S13186/1−S13186/3.
(179) Kelly, B. T. *Carbon* **1972**, *10*, 429–433.
(180) Nelson, J. B.; Riley, D. P. *Proc. Phys. Soc., London* **1945**, *57*, 477.
(181) Osman, M. A.; Mittal, V.; Morbidelli, M.; Suter, U. W. *Macromolecules* **2003**, *36*, 9851–9858.

(182) Lape, N. K.; Nuxoll, E. E.; Cussler, E. L. *J. Membr. Sci.* **2004**, *236*, 29–37.
(183) Xu, Y.; Hong, W.; Bai, H.; Li, C.; Shi, G. *Carbon* **2009**, *47*, 3538–3543.
(184) Villar-Rodil, S.; Paredes, J. I.; Martinez-Alonso, A.; Tascon, J. M. D. *J. Mater. Chem.* **2009**, *19*, 3591–3593.
(185) Kashiwagi, T.; Du, F.; Douglas, J. F.; Winey, K. I.; Harris, R. H.; Shields, J. R. *Nature Mater.* **2005**, *4*, 928–933.
(186) Kashiwagi, T.; Mu, M.; Winey, K.; Cipriano, B.; Raghavan, S. R.; Pack, S.; Rafailovich, M.; Yang, Y.; Grulke, E.; Shields, J.; Harris, R.; Douglas, J. *Polymer* **2008**, *49*, 4358–4368.
(187) Graphene-Industries Raw graphene, Devices and Membranes for Sale, grapheneindustries.com/?Sample+Catalog, accessed on June 14, 2010.
(188) Baytubes, www.baytubes.com, accessed on June 14, 2010.
(189) SouthWest NanoTechnologies, www.swentnano.com, accessed on June 14, 2010.
(190) Vorbeck Materials, www.vorbeck.com, accessed on June 14, 2010.
(191) Angstron Materials, www.angstronmaterials.com, accessed on June 14, 2010.
(192) Magrez, A.; Kasas, S.; Salicio, V.; Pasquier, N.; Seo, J. W.; Celio, M.; Catsicas, S.; Schwaller, B.; Forro, L. *Nano Lett.* **2006**, *6*, 1121–1125.
(193) Panessa-Warren, B. J.; Warren, J. B.; Wong, S. S.; Misewich, J. A. *J. Phys.: Condens. Matter* **2006**, *18*, S2185–S2201.
(194) Yang, D.; Velamakanni, A.; Bozoklu, G.; Park, S.; Stoller, M.; Piner, R. D.; Stankovich, S.; Jung, I.; Field, D. A.; Ventrice, C. A., Jr.; Ruoff, R. S. *Carbon* **2009**, *47*, 145–152.
(195) Li, Z.; Zhang, W.; Luo, Y.; Yang, J.; Hou, J. G. *J. Am. Chem. Soc.* **2009**, *131*, 6320–6321.
(196) Kim, M. C.; Hwang, G. S.; Ruoff, R. S. *J. Chem. Phys.* **2009**, *131*, 064704/1–064704/5.
(197) Thostenson, E. T.; Chou, T.-W. *J. Phys. D: Appl. Phys.* **2002**, *35*, L77–L80.
(198) Haggenmueller, R.; Gommans, H. H.; Rinzler, A. G.; Fischer, J. E.; Winey, K. I. *Chem. Phys. Lett.* **2000**, *330*, 219–225.
(199) Hong, C.-M.; Kim, J.; Jana, S. C. *Polym. Eng. Sci.* **2004**, *44*, 2101–2109.
(200) Kharchenko, S. B.; Douglas, J. F.; Obrzut, J.; Grulke, E. A.; Migler, K. B. *Nature Mater.* **2004**, *3*, 564–568.
(201) Obrzut, J.; Douglas, J. F.; Kharchenko, S. B.; Migler, K. B. *Phys. Rev. B: Condens. Matter* **2007**, *76*, 195420/1–195420/9.
(202) Du, F.; Fischer, J. E.; Winey, K. I. *Phys. Rev. B: Condens. Matter* **2005**, *72*, 121404/1–121404/4.
(203) Hull, D.; Clyne, T. W. *An Introduction to Composite Materials*, 2nd ed.; Cambridge University Press: London, 1996.
(204) Bharadwaj, R. K. *Macromolecules* **2001**, *34*, 9189–9192.
(205) Vaia, R. A.; Maguire, J. F. *Chem. Mater.* **2007**, *19*, 2736–2751.
(206) Mamedov, A. A.; Kotov, N. A.; Prato, M.; Guldi, D. M.; Wicksted, J. P.; Hirsch, A. *Nature Mater.* **2002**, *1*, 190–194.
(207) Velasco-Santos, C.; Martinez-Hernandez, A. L.; Fisher, F. T.; Ruoff, R.; Castano, V. M. *Chem. Mater.* **2003**, *15*, 4470–4475.
(208) Konatham, D.; Striolo, A. *Appl. Phys. Lett.* **2009**, *95*, 163105/1–163105/3.
(209) Zammarano, M.; Kramer, R. H.; Harris, R., Jr.; Ohlemiller, T. J.; Shields, J. R.; Rahatekar, S. S.; Lacerda, S.; Gilman, J. W. *Polym. Adv. Technol.* **2008**, *19*, 588–595.
(210) Thirumal, M.; Khastgir, D.; Singha, N. K.; Manjunath, B. S.; Naik, Y. P. *J. Appl. Polym. Sci.* **2008**, *110*, 2586–2594.
(211) Koerner, H.; Price, G.; Pearce, N. A.; Alexander, M.; Vaia, R. A. *Nature Mater.* **2004**, *3*, 115–120.
(212) Al-Saleh, M. H.; Sundararaj, U. *Macromol. Mater. Eng.* **2008**, *293*, 789.
(213) Mather, P. J.; Thomas, K. M. *J. Mater. Sci.* **1997**, *32*, 1711–1715.
(214) Kobashi, K.; Villmow, T.; Andres, T.; Haeussler, L.; Poetschke, P. *Smart Mater. Struct.* **2009**, *18*, 035008/1–035008/15.
(215) Wang, X.; Fu, X.; Chung, D. D. L. *J. Mater. Res.* **1999**, *14*, 790–802.
(216) Ahir, S. V.; Terentjev, E. M. *Nature Mater.* **2005**, *4*, 491–495.
(217) Baughman, R. H.; Cui, C.; Zakhidov, A. A.; Iqbal, Z.; Barisci, J. N.; Spinks, G. M.; Wallace, G. G.; Mazzoldi, A.; De Rossi, d.; Rinzler, A. G.; Jaschinski, O.; Roth, S.; Kertesz, M. *Science* **1999**, *284*, 1340–1344.
(218) Nair, R. R.; Blake, P.; Grigorenko, A. N.; Novoselov, K. S.; Booth, T. J.; Stauber, T.; Peres, N. M. R.; Geim, A. K. *Science* **2008**, *320*, 1308.
(219) Kim, K. S.; Zhao, Y.; Jang, H.; Lee, S. Y.; Kim, J. M.; Kim, K. S.; Ahn, J.-H.; Kim, P.; Choi, J.-Y.; Hong, B. H. *Nature* **2009**, *457*, 706–710.
(220) Eda, G.; Fanchini, G.; Chhowalla, M. *Nature Nanotechnol.* **2008**, *3*, 270–274.
(221) Tung, V. C.; Chen, L.-M.; Allen, M. J.; Wassei, J. K.; Nelson, K.; Kaner, R. B.; Yang, Y. *Nano Lett.* **2009**, *9*, 1949–1955.
(222) Blake, P.; Brimicombe, P. D.; Nair, R. R.; Booth, T. J.; Jiang, D.; Schedin, F.; Ponomarenko, L. A.; Morozov, S. V.; Gleeson, H. F.; Hill, E. W.; Geim, A. K.; Novoselov, K. S. *Nano Lett.* **2008**, *8*, 1704–1708.
(223) Becerril, H. A.; Mao, J.; Liu, Z.; Stoltenberg, R. M.; Bao, Z.; Chen, Y. *ACS Nano* **2008**, *2*, 463–470.
(224) Liang, J.; Huang, Y.; Zhang, L.; Wang, Y.; Ma, Y.; Guo, T.; Chen, Y. *Adv. Funct. Mater.* **2009**, *19*, 2297–2302.
(225) Fang, M.; Wang, K.; Lu, H.; Yang, Y.; Nutt, S. *J. Mater. Chem.* **2009**, *19*, 7098–7105.
(226) Cai, D.; Yusoh, K.; Song, M. *Nanotechnology* **2009**, *20*, 085712/1–085712/5.
(227) Mack, J. J.; Viculis, L. M.; Ali, A.; Luoh, R.; Yang, G.; Hahn, H. T.; Ko, F. K.; Kaner, R. B. *Adv. Mater.* **2005**, *17*, 77–80.
(228) Zhang, L.; Liang, J.; Huang, Y.; Ma, Y.; Wang, Y.; Chen, Y. *Carbon* **2009**, *47*, 3365–3368.